CHALMERS
UNIVERSITY OF TECHNOLOGY

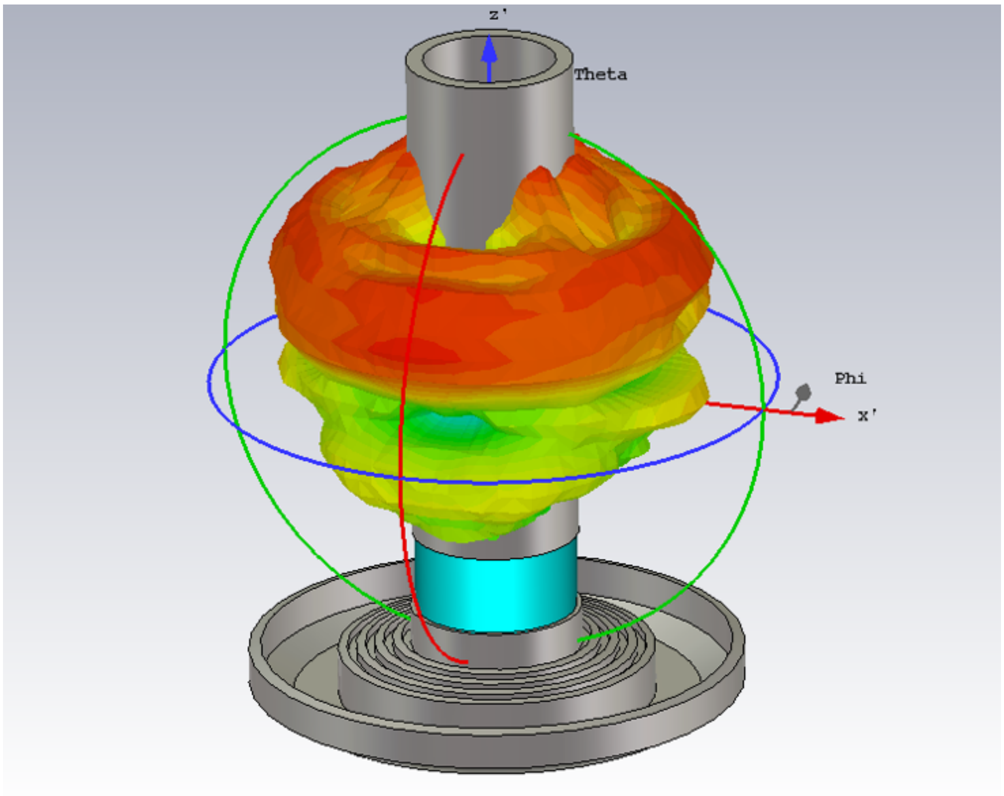

Dual Band Hat Fed Antenna for 5G Backhauling

Master's thesis in Wireless, photonics and space engineering

MARCUS ANDERSSON

Department of Electrical Engieneering
CHALMERS UNIVERSITY OF TECHNOLOGY
Gothenburg, Sweden 2019

MASTER'S THESIS 2019

Dual Band Hat Fed Antenna for 5G Backhauling

MARCUS ANDERSSON

Department of Electrical Engieneering
Division of Communication and Antenna Systems
Antenna Systems Group
CHALMERS UNIVERSITY OF TECHNOLOGY
Gothenburg, Sweden 2019

Dual Band Hat Fed Antenna for 5G Backhauling MARCUS ANDERSSON

Supervisor: Tomas Östling, CTO, LEAX Arkivator Telecom AB
Supervisor: Guang Yang, LEAX Arkivator Telecom AB
Supervisor: Ashraf Uz Zaman, Assistant Professor, Department of Electrical Engineering
Examiner: Jian Yang, Professor, Department of Electrical Engineering

Master's Thesis 2019
Department of Electrical Engineering
Division of Communication and Antenna Systems
Antenna Systems Group
Chalmers University of Technology
SE-412 96 Gothenburg
Telephone +46 31 772 1000

Cover: Model of a hat feed with field radiation pattern. Modelled and simulated in CST.

Typeset in LaTeX
Gothenburg, Sweden 2019

Dual Band Hat Fed Antenna for 5G Backhauling
A Subtitle that can be Very Much Longer if Necessary
MARCUS ANDERSSON
Department of Electrical Engineering
Chalmers University of Technology

Abstract

The need of higher data rates in mobile communication has accelerated the development of the fifth generation cellular network (5G). Higher speed base stations set requirements for the backhauling system. Therefor, higher frequency bands have been allocated for this purpose. Higher frequencies have the disadvantage of being sensitive to weather, and therefore a dual-band (high and low frequency) system is desired.

This project investigates the possibility to modify an existing hat-fed reflector antenna to have dual-band support with a lower frequency band (17.7-19.7 GHz) *or* (24.5-26.5 GHz) and a higher frequency band, E-band (71-76, and 81-86 GHz).

A original hat fed antenna from LEAX Arkivator Telecom AB, optimized for 18 GHz band, has been parameterized. The parameters has then been modified. Two different models was achieved. The first model, optimized for dual-band 18 GHz *and* E-band with a reflection coefficient better than -17 dB and -11 dB respectively. The aperture efficiency was better than 33 % and 53 % respectively. The second model, optimized for 24 GHz and E-band had a reflection coefficient better than -17 dB and -15 dB respectively. The aperture efficiency was better than 53 % and 44 % respectively. Both models have acceptable performance in the case of reflection coefficient, but the aperture efficiency is poor for the first model at 18 GHz band. This was due to bad polarization efficiency.

Keywords: hat feed, hat fed antenna, dual-band feed, 18 GHz band, 24 GHz band, E-band 5G wireless communication system, reflector antenna

Acknowledgements

This thesis was done at Chalmers University of Technology for the company LEAX Arkivator Telecom AB. I have cooperated with Tomas Östling (LEAX), Guang Yang (LEAX), Ashraf Uz Zaman (Chalmers), and Jian Yang (Chalmers).

I want to thank all for their assistance during the project, through weekly meetings and mail contact. Thanks to Guang Yang for help with comparing results with V2D software, and thanks to Tomas, Ashraf and Jian for your help with finding the next work step, inter alia by staring at fields.

I also want to thank other people at the antenna group I have met (and rececived help from) during the work on my thesis. Thanks to my room mate for the first two months, Prabhat Khanal, who helped me out with simulations in CST.

Marcus Andersson, Gothenburg, December 2019

Contents

List of Figures

List of Tables

1
Introduction

1.1 Background

The fifth generation (5G) cellular network is under development, and has requirements of higher data rate, higher availability, and lower latency. A critical part of a mobile network is to establish links between base stations, either through wire, or wireless. Wired links are known for stability and high bandwidth, but are compared to wireless links expensive and not as flexible. To obtain higher bandwidth for wireless links, higher frequency bands have been allocated. A problem using higher frequencies though, is its sensitivity to weather conditions, especially rain. In certain weather conditions the availability can be drastically worse. One solution to ensure the availability is to make use of two frequency bands (dual-band), one lower that has higher availability, and one higher that, when available, will provide higher data-rate. Also, this solution is used to simply improve the capacity of the base station.
A challenge is to develop compact dual-band systems, since it needs to be optimized for two widely spaced frequency bands. In the case of using reflector antennas, for the sake of compactness, it is desirable to use one single antenna that is compatible for both frequency bands. To have high dual-band efficiency in such an antenna, a dual-band compatible feed is needed. One type of feed that can be used, are the so called *hat feed*.

1.2 Task

This project aims to investigate the possibility to model a hat fed antenna with dual-band support for 18 GHz band (17.7-19.7 GHz) *or* 24 GHz band (24.5-26.5 GHz) and E-band (71-76 and 81-86 GHz).

1.3 Scope

This work is limited to find a computer model, validation of a manufactured model is outside the scope. The model is based on an existing model from LEAX Arkiator, which supports dual-polarization for 18 GHz. This project only investigates single polarization and excitation of the hat feed is not covered. Since the time for this project was limited, only the feed was simulated, i.e. without a reflector.

1.3.1 Comment on simulation time

The simulation software used was CST, which is a full 3D electromagnetic solver. As solution the finite difference time domain (FDTD) method was used, which is preferable when simulating complex structures. Still, because of the relatively high frequency used (maximum of 86 GHz), each simulation could take up to 2.5 hours.

2
Theory

In this chapter, theory needed to understand this project is presented. Electromagnetics is rather complex, so this chapter will only touch an ounce of it. For a more detailed explanation of electromagnetic theory, the reader is referred to books like [1] and [2].

2.1 Antenna theory

In this section, basics to antenna theory are explained, with a focus on the hat fed reflector antenna.

2.1.1 Electromagnetic field and plane waves

The theory behind electromagnetics (EM) was developed during the 19:th century, in 1873 Maxwell summarized the theory with what is called Maxwell's equations. Hertz verified this theory experimentally in 1893. The knowledge of EM has resulted in many useful applications, such as transmission lines, waveguides, fiber optics and antennas. With this short introduction the author of this thesis wants to give a big thanks to the scientists in the past that made all these applications possible.

A electromagnetic field from an antenna is generated by current source with fast electric or magnetic variations.For the study of such field, it is easiest to consider the *steady sinusoidal time varying* (also called time-harmonic) source function

$$\cos(\omega t + \Phi) = \Re\Big\{e^{j(\omega t + \Phi)}\Big\}, \tag{2.1}$$

where ϕ is the phase and ω the angular frequency. A field induced by time-harmonic sources will also be a time-harmonic. Such a field is called the *instantaneous field*

$$\overrightarrow{E}(x, y, z, t) = \Re\Big\{\boldsymbol{E}(x, y, z)e^{j\omega t}\Big\}, \tag{2.2}$$

where $\boldsymbol{E}$ is a time-harmonic field. Because the field is propagating in radial direction from the antenna, it can far away from the antenna be considered as plane waves. Where a plane wave is described as infinite planes with constant phase and amplitude, parallel to each other. True plane waves does not physically exist but is a good approximation of a field far from its source. Considering the time-harmonic field being a plane wave in free space, a wave propagating in z-direction is described as

$$\boldsymbol{E} = [E_x\hat{\boldsymbol{x}} + E_y\hat{\boldsymbol{y}}]e^{-jkz}. \tag{2.3}$$

In the rest of this Chapter, plane waves in $\hat{\boldsymbol{z}}$-direction are assumed, see Figure 2.1 The H-field is

$$\boldsymbol{H} = \frac{1}{\eta}\hat{z} \times \boldsymbol{E} = \frac{1}{\eta}[-E_y\hat{\boldsymbol{x}} + E_x\hat{\boldsymbol{y}}]e^{-jkz}, \tag{2.4}$$

where $\eta = 377\ \Omega$ is the free space wave impedance, and $k = \frac{2\pi}{\lambda}$ is the wave number.

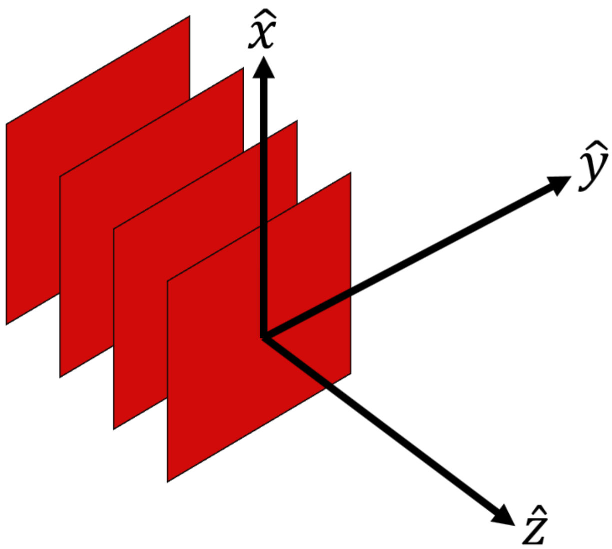

Figure 2.1: Plane wave in $\hat{\boldsymbol{z}}$-direction and infinite xy-plane. This type of wave is considered in the rest of this Chapter.

2.1.2 Hat fed antenna

In this thesis, a *hat fed antenna* are to be designed. It is a reflector antenna fed by a so called hat feed. A general hat fed antenna is shown in Figure 2.2. The feed consists of three main parts; a circular waveguide (the *neck*), a dielectric *head*, and a metallic *hat*. The hat feed was invented and patented by Per-Simon Kildal [3]. Later it has been further developed by many researchers over the world [4]–[14]. It has the feature of being self-supported, which compared to reflector antennas with supported feeds has lower blockage loss. The radiation from a hat feed has a so called ring focus, which means that the focus is not directed to one certain point, but rather in several points which creates a "ring of focuses". This introduces phase error, which causes loss. Luckily, this can be resolved by shaping the reflector according to the method found in [15]. The main advantages of the hat feed is that it has low cross polarization level, low sidelobes, low blockage, and low ohmic loss [16].

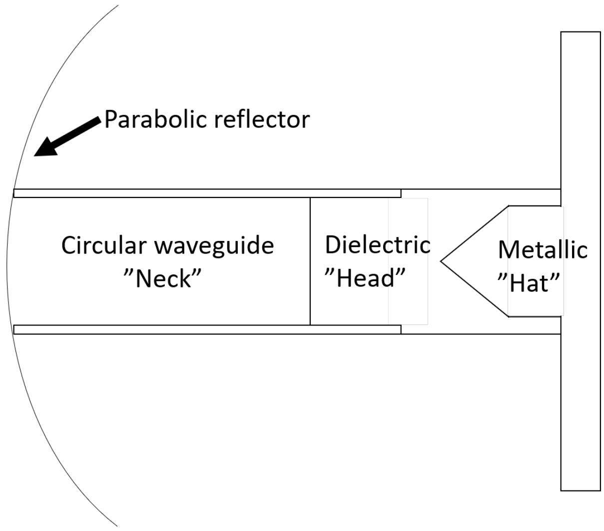

Figure 2.2: The hat feed is divided into three main parts; the neck, head, and hat.

2.1.3 Parabolic reflector antenna and aperture efficiency

A parabolic reflector antenna is a unit which reflects electromagnetic fields and has the advantage of high efficiency *and* directivity. This makes it suitable for point-to-point communication, which is an important part in the mobile network architecture. The maximum gain is found as

$$G_{max} = \frac{4\pi f^2}{c^2} A_{eff}, \tag{2.5}$$

where f is the carrier frequency, c is the speed of light in air, and A_{eff} is the effective aperture area of the reflector. This can further be described as

$$A_{eff} = Ae_{ap}, \tag{2.6}$$

where A is the physical aperture area of the reflector, and e_{ap} is the total efficiency factor of the antenna. The total efficiency can be divided into several efficiency factors, namely; spillover (e_{sp}), illumination (e_{ill}), polarization (e_{pol}), and phase (e_{ϕ}) efficiency. In the case of $BOR1$ antennas (like the hat feed) a BOR1 efficiency (e_{BOR1}) is also contributing to the aperture efficiency. Thus the total aperture efficiency is found as [17]–[19]

$$e_{ap} = e_{sp} e_{ill} e_{pol} e_{\phi} e_{BOR1}. \tag{2.7}$$

Brief explanations of the *sub-efficiencies* are found in Table 2.1

Table 2.1: Short explanation of different efficiencies.

Efficiency	Reason for loss
e_{BOR1}	Far field power loss caused by higher order variations in azimuth.
e_{sp}	Part of the radiation field is not included in the subtended angle (see Figure 2.3).
e_{pol}	Co-polar field vs total power that illuminates the reflector.
e_{ill}	The hole reflector is not illuminated.
e_{ϕ}	Far-field phase error, which is caused when the phase center is not placed correctly.

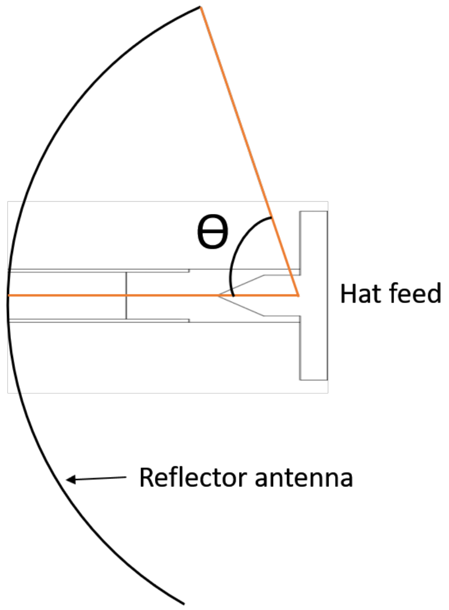

Figure 2.3: The figure illustrates the subtended angle of a reflector antenna, the angle between the edge of the reflector to the feed.

The approximations of the sub-efficiencies in this project is calculated in the same way as in [20].

2.1.4 Polarization

For plane waves in vacuum, the electric and magnetic fields are orthogonal. Further in this section such a wave is assumed. A wave **E** propagating in z-direction is often divided into two components, the x-component E_x (x-polarized), and the y-component E_y (y-polarized). Those two orthogonal polarizations can be used simultaneously to increase the transmission capacity in a data link. In theory the speed of the link should be twice as fast. But to achieve this, there need to be good isolation between the two polarizations, thus the interference between them need to be low. Each polarization needs to be excited separately, the one that is excited (and desired) is called the *co-polar* polarization, and the undesired is called *cross-polar*. In general these are defined as orthogonal to one another, which mathematically means that

$$\hat{\boldsymbol{co}} \cdot \hat{\boldsymbol{co}}^* = 1, \qquad \hat{\boldsymbol{co}} \cdot \hat{\boldsymbol{xp}}^* = 0, \tag{2.8}$$

$$\hat{\boldsymbol{xp}} \cdot \hat{\boldsymbol{xp}}^* = 1, \qquad \hat{\boldsymbol{xp}} \cdot \hat{\boldsymbol{co}}^* = 0. \tag{2.9}$$

Now, by taking the scalar product between an E-field $\boldsymbol{E_t}$ and $\hat{\boldsymbol{co}}^*$ or $\hat{\boldsymbol{xp}}^*$ the co- and cross-polar field components are found respectively, i.e.

$$E_{co} = \boldsymbol{E}_t \cdot \hat{\boldsymbol{co}}^* \qquad E_{xp} = \boldsymbol{E}_t \cdot \hat{\boldsymbol{xp}}^* \tag{2.10}$$

Having introduced the concept of co- and cross-polar polarization, a general polarized plane wave in vacuum can now be described as

$$\mathbf{E} = (E_{co}\hat{\boldsymbol{co}} + E_{xp}\hat{\boldsymbol{xp}})e^{-jkz}, \tag{2.11}$$

where $\hat{\boldsymbol{co}}$ and $\hat{\boldsymbol{xp}}$ are both orthogonal to the propagating direction $\hat{\boldsymbol{z}}$.
There exists two main types of polarization; 1)*linear polarization*, in which the electric field is varying in one plane and 2) *circular polarization*, where the electric field is propagating in the shape of a corkscrew. If a link is established between two antennas with linear polarization, they need to be aligned, otherwise power loss is introduced. This is not the case for circular polarized antennas, which makes them more flexible. However, in the case of a point-to-point link, antenna alignment is rather simple.

Co-polar and cross-polar example

If for instance the x-component (linear polarization in $\hat{\boldsymbol{x}}$-direction) of the E-field is the desired polarization, then

$$\hat{\boldsymbol{co}} = \hat{\boldsymbol{x}} \textit{ and } \hat{\boldsymbol{xp}} = \hat{\boldsymbol{y}}. \tag{2.12}$$

Circular polarization can either be *right-hand circular* (RHC) or *left-hand circular* (LHC). The co- and cross-polar for RHC polarization is

$$\hat{\boldsymbol{co}} = \frac{(\hat{\boldsymbol{x}} - j\hat{\boldsymbol{y}})}{\sqrt{2}}, \qquad \hat{\boldsymbol{xp}} = \frac{(\hat{\boldsymbol{x}} + j\hat{\boldsymbol{y}})}{\sqrt{2}}, \tag{2.13}$$

and for LHC polarization reversed

$$\hat{\boldsymbol{co}} = \frac{(\hat{\boldsymbol{x}} + j\hat{\boldsymbol{y}})}{\sqrt{2}}, \qquad \hat{\boldsymbol{xp}} = \frac{(\hat{\boldsymbol{x}} - j\hat{\boldsymbol{y}})}{\sqrt{2}}. \tag{2.14}$$

2.1.5 Radiation and far-field

In free-space, the far-field is defined in a point, at a certain distance from the antenna. This point appears where the shape of the radiation pattern remains unchanged independently on distance. If the distance to this point is $\boldsymbol{r}$, the field variations can be separated to

$$E(\boldsymbol{r}) = \frac{G(\hat{\boldsymbol{r}})e^{-}jkr}{r}, \tag{2.15}$$

where $G(\hat{\boldsymbol{r}})$ is called *far-field function* or *radiation field function*.
For an antenna with diameter D radiating at a frequency f, the distance $\boldsymbol{r}$ is often defined as

$$\boldsymbol{r} \geq \frac{2D^2 f}{c}, \tag{2.16}$$

since this condition ensures that the field is in the *far-field region*.

2.2 Microwave properties

Here, circular waveguides and dielectric materials are explained. This since their both important parts of the hat feed investigated in this thesis.

2.2.1 Circular waveguide

The neck of the hat antenna is a simple circular waveguide, here its propagation properties are explained.
A waveguide is a type of transmission line, in which electromagnetic waves propagates. The two main types of waveguides are rectangular waveguides *and* circular waveguides, here the later is considered. They consists most often of a metallic material (e.g. copper or brass), and are filled with a propagation medium. The medium can either be air (hollow waveguide) or a dielectric material. Two types of travelling waves are present in a waveguide, the *transverse electric* (TE), and the *transverse magnetic* (TM) waves, which may propagate at the same time. What differs these two types are the presence of magnetic (for TE) or electric (for TM) field components. Moreover, there are several types of TE and TM waves, called *modes* which may propagate in a waveguide. The presence of a mode can be determined by a cutoff frequency

$$f_{c,mn} = \frac{p_{mn}}{2\pi a\sqrt{\mu\epsilon}}, \tag{2.17}$$

where mn is the mode number, a is the inside radius of the waveguide, μ the permeability, ϵ the permitivity, and p_{mn} is Bessel function solutions which can be found for TE and TM modes in Table 2.2 and 2.3. Considering Equation (2.17), each mode has its own cutoff frequency. The mn-mode is present when the frequency of the excited wave is greater then the mn-mode cutoff frequency. For a certain waveguide it is seen from Equation (2.17) that the first mode that appears when sweeping from lower to higher frequency, is the mode which has the lowest value of the Bessel function, the TE_{11}-mode. This is called the fundamental mode, and will be the only present mode when the excited frequency is lower than the frequency of the next mode, the TM_{01}-mode. When the frequency is further increased, more modes will appear in the waveguide.

Table 2.2: Bessel functions for TE-mode.

n	p_{n1}	p_{n2}	p_{n3}
0	3.832	7.016	10.174
1	1.841	5.331	8.536
2	3.054	6.706	9.970

Table 2.3: Bessel functions for TM-mode.

n	p_{n1}	p_{n2}	p_{n3}
0	2.405	5.520	8.654
1	3.832	7.016	10.174
2	5.136	8.417	11.620

2.2.2 Dielectric

A material is considered to be a dielectric if it compared to a metal has low conductivity. In turn this gives a material with high polarization density, $\boldsymbol{P}$. This quantity is defined as

$$\boldsymbol{P} = \epsilon\chi_e\boldsymbol{E}, \tag{2.18}$$

where χ_e is called the electric susceptibility. The dielectric constant,ϵ_r is defined as

$$\epsilon_r = 1 + \chi_e = \frac{\epsilon}{\epsilon_0}, \tag{2.19}$$

where ϵ_0 is the vacuum permittivity. These equations holds only for a linear, homogeneous, and isotropic medium, which in reality is not the case, even though it can be a good approximation [1]. In the case of a lossy medium the dielectric constant is a complex quantity as

$$\epsilon = \epsilon^{'} - j\epsilon^{''}, \tag{2.20}$$

where $\epsilon^{'} = \epsilon_r\epsilon_0$ and $\epsilon^{''} = \epsilon^{'} j \tan\delta$. $\tan\delta$ is a material property called *loss tangent*[2].

2.3 Computer simulation

Two simulation techniques used in this project is explained briefly in this section. The *Finite Difference Time Domain method* (FDTD), and the use of *symmetry planes*.

2.3.1 Finite Difference Time Domain Method

This explanation will not go through the mathematics behind, but just the basic idea. For a more fundamental explanation, the reader is referred to books on the subject, for instance [21]. FDTD is a numerical method that aims to find approximate finite solutions to partial differential equations (PDE), such as Maxwell's equations. Using the method for electromagnetic simulations, the idea is to calculate the E and H field of discrete points in a defined region, called the *computational domain*. The result is an approximation of the electromagnetic field in that domain.

2.3.2 Symmetry planes

The hat feed used in this project is rotational symmetric. This opens the possibility to use so called *symmetry planes* to speed up the simulations. In CST this is done by defining the planes in which the E and H fields has no tangential components. Each symmetry plane will reduce the simulation time by half. In the case of the rotational symmetric hat feed, two symmetry planes can be defined, and therefor reduce the simulation time by a quarter.

3

Design of dual-band antenna models

One of the critical parts of this project was to establish a modeling strategy. The proceeding is explained in this chapter. The modeling and simulations were done in the 3D electromagnetic simulation software *CST Studio Suite*, further referred as CST.

3.1 Goals

Before modeling, some requirements on the performance were defined. Two parameters was considered here; 1) *return loss*, which is the power loss due to reflections back to the input, and 2) *aperture efficiency*, which was explained in Chapter 2.1.3. The return loss goal for 18 GHz was set to -20 dB, and for higher frequency band -15 dB. The goal for aperture efficiency was to achieve at least 50 % for both frequency bands.

3.2 Modeling

Designing a hat feed from scratch requires a lot of computer power and time. Therefor, in this project, the idea was to modify an already existing 18 GHz antenna from LEAX Arkivator Telecom AB, to make it work also for E-band (Model 1) *or* for 24 GHz band and E-band (Model 2). In the first step, the initial model was modeled in CST and simulated for all bands. This model is shown in Figure 3.1, and its performance in terms of return loss and aperture efficiency for all bands are shown in Figure 3.2-3.4 and Table 3.1-3.3. During the project work, trials with a upscaled model for 18 GHz and E-band was also done. It showed great performance in terms of return loss, but poor aperture efficiency due to strong overmodes in the waveguide tube.

The modeling idea was to find how a change in different design parameters would affect the antenna performance for different bands. The reflections are mainly caused by the dielectric head, thus it was parametrized. Also, the neck was shortened to speed up the simulations.

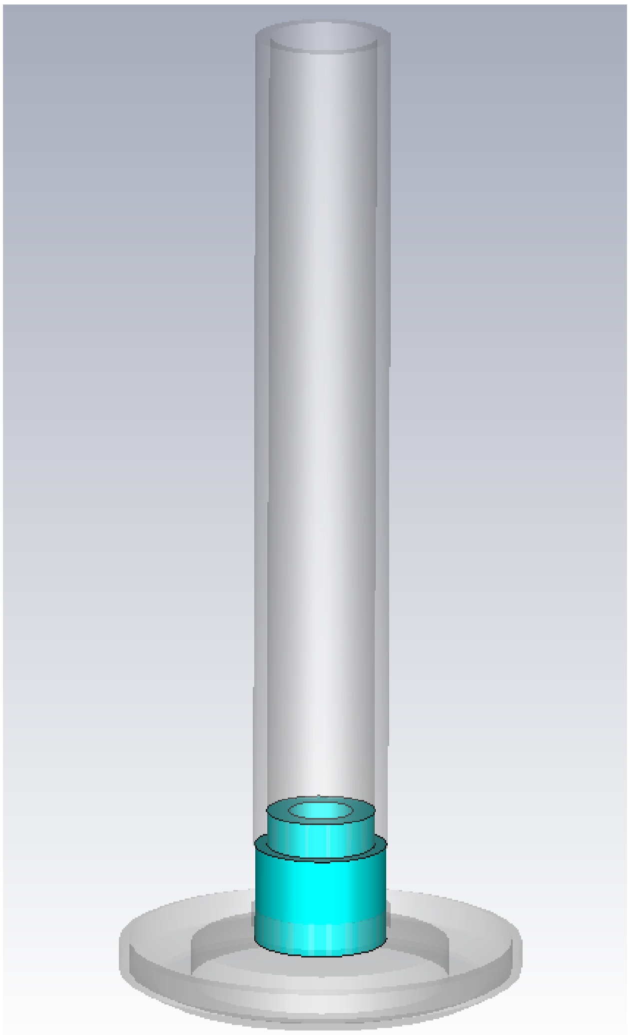

Figure 3.1: Model in CST of the original 18 GHz band hat feed from Arkivator AB.

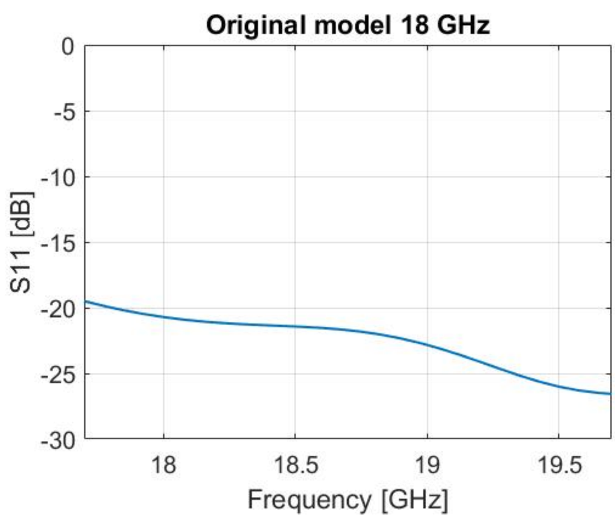

Figure 3.2: Return loss for 18 GHz band of the original model.

Table 3.1: Efficiencies and total aperture efficiency for the original model at 18 GHz.

Freq [GHz]	e_{BOR1}	e_{sp}	e_{ill}	e_{pol}	$\boldsymbol{e_{ap}}$
18	99 %	96 %	74 %	97 %	**69%**

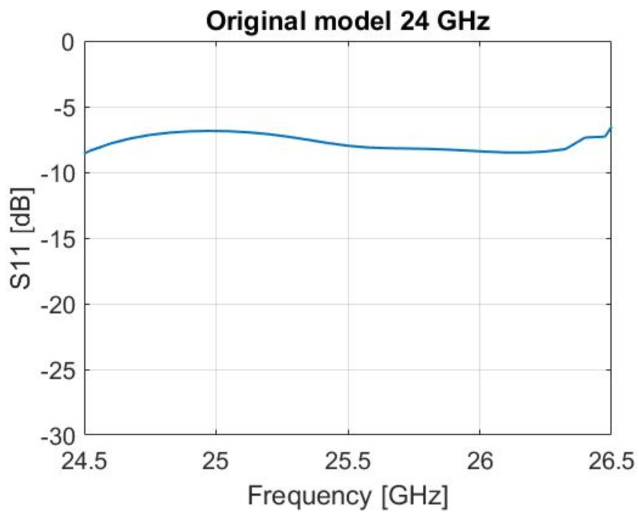

Figure 3.3: Return loss for 24 GHz band of the original model.

Table 3.2: Efficiencies and total aperture efficiency for the original model at 24 GHz band.

Freq [GHz]	e_{BOR1}	e_{sp}	e_{ill}	e_{pol}	$\boldsymbol{e_{ap}}$
24.5	99 %	96 %	81 %	76 %	**59%**
26.5	99 %	90 %	69 %	60 %	**37%**

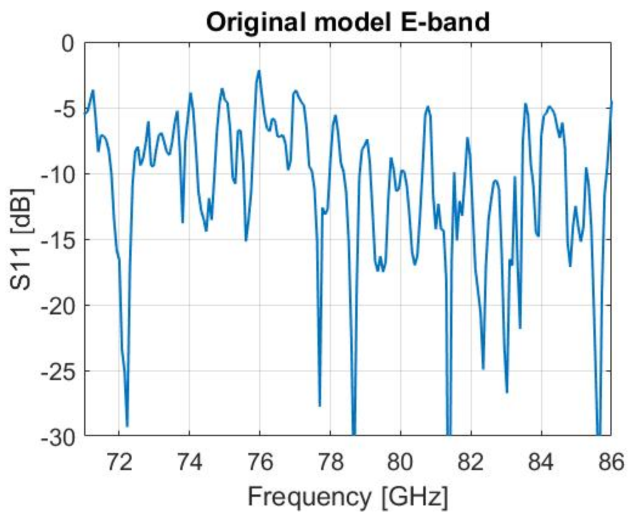

Figure 3.4: Return loss for E-band of the original model.

Table 3.3: Efficiencies and total aperture efficiency for the original model at E-band.

Freq [GHz]	e_{BOR1}	e_{sp}	e_{ill}	e_{pol}	$\boldsymbol{e_{ap}}$
71	99 %	95 %	64 %	50 %	**30%**
81	98 %	98 %	41 %	55 %	**22%**
86	97 %	98 %	71 %	58 %	**39%**

3.2.1 Dielectric head and corrugations

As seen in Figure 3.4, the return loss was overall bad for E-band. To reduce the reflections, a smooth transition in the form of a cone was introduced. Also, to reduce the cross-polar level, corrugations for E-band was added as in [22]. The corrugations are $\frac{\lambda}{4}$ deep, where λ is the wavelength for 80 GHz. This modified model is shown in Figure 3.5. The strategy now was to optimize the dielectric head shape to have low return loss, and then look at the aperture efficiency. This was done by running simulation sweeps with small changes (in terms of E-band wavelength) of the parameter values. The dielectric head parameters are shown in Figure 3.6. A simulation sweep was also performed for the dielectric constant of the head material, to investigate its effects on the return loss.

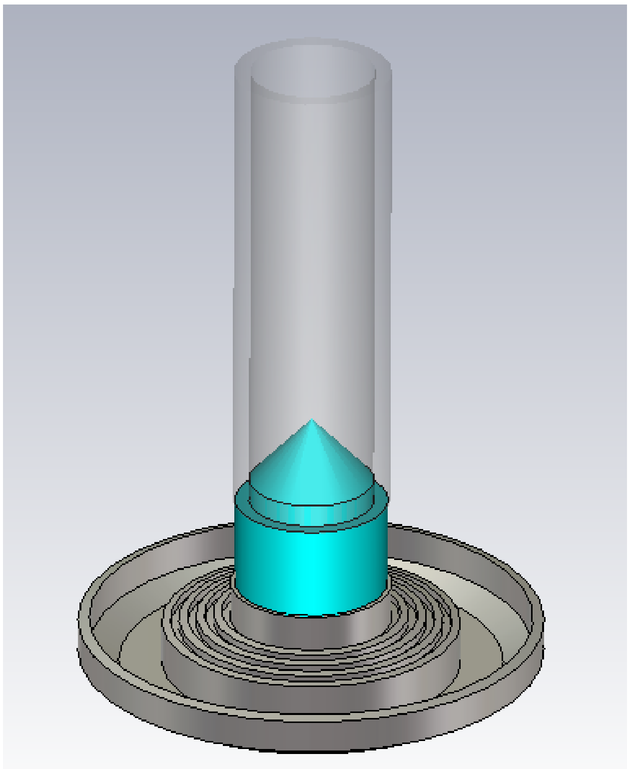

Figure 3.5: Model where the dielectric head was modified to a cone, to have a more smooth transition for E-band. Corrugations were added to prevent radiation leakage.

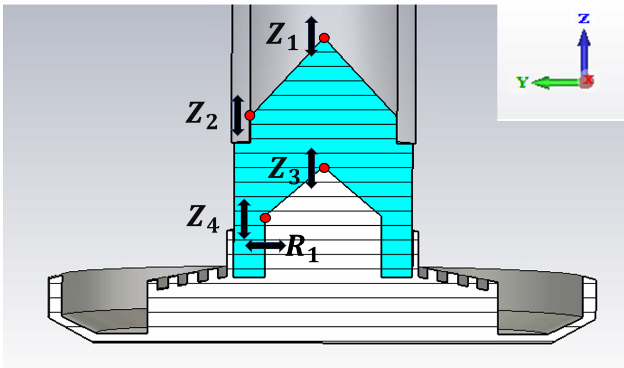

Figure 3.6: Parametrizing of the dielctric head.

3.2.1.1 Head parameter sweeps for 18 GHz band and E-band

Here, the return loss of the parameter sweeps are shown. The parametrized model in Figure 3.6 is the *base model*. *Increase* and *decrease* data in the plots refers to a small increase and decrease respectively, compared to the base model. The plots was studied to get a sense of how changes of the parameter values affects the return loss.

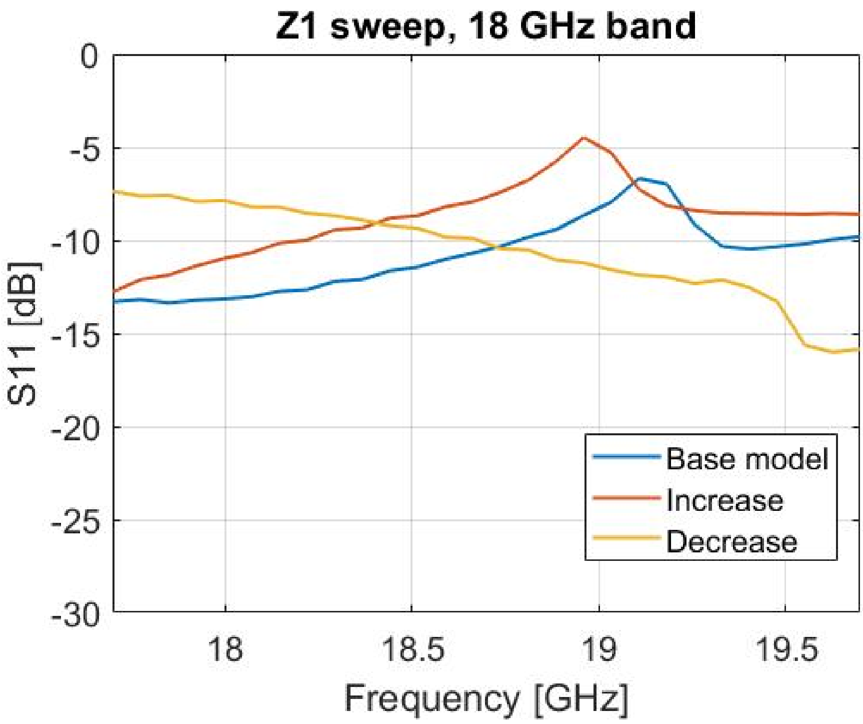

Figure 3.7: Z1 parameter sweep for 18 GHz band.

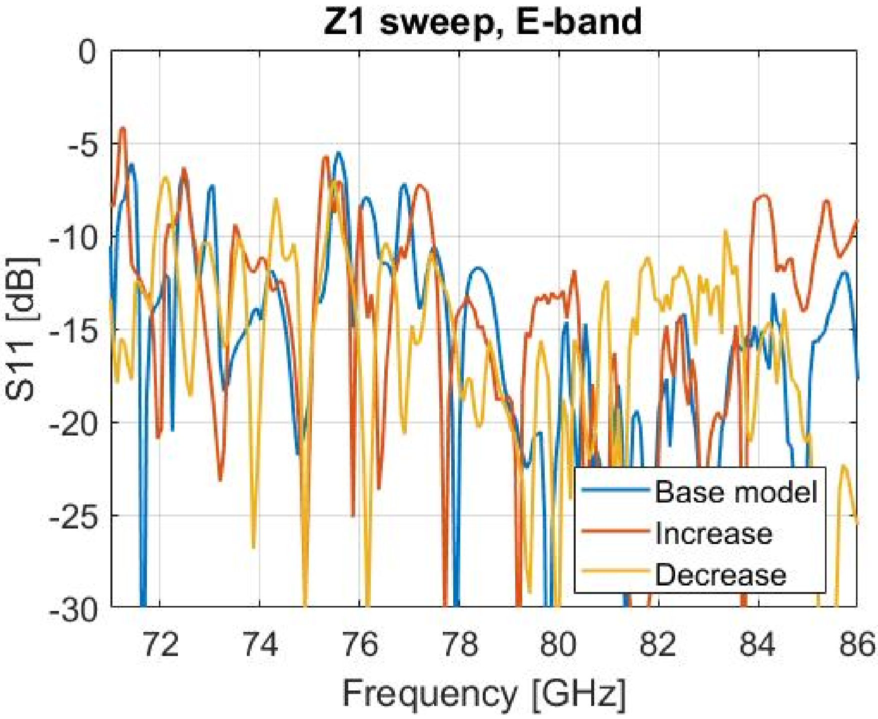

Figure 3.8: Z1 parameter sweep for E-band.

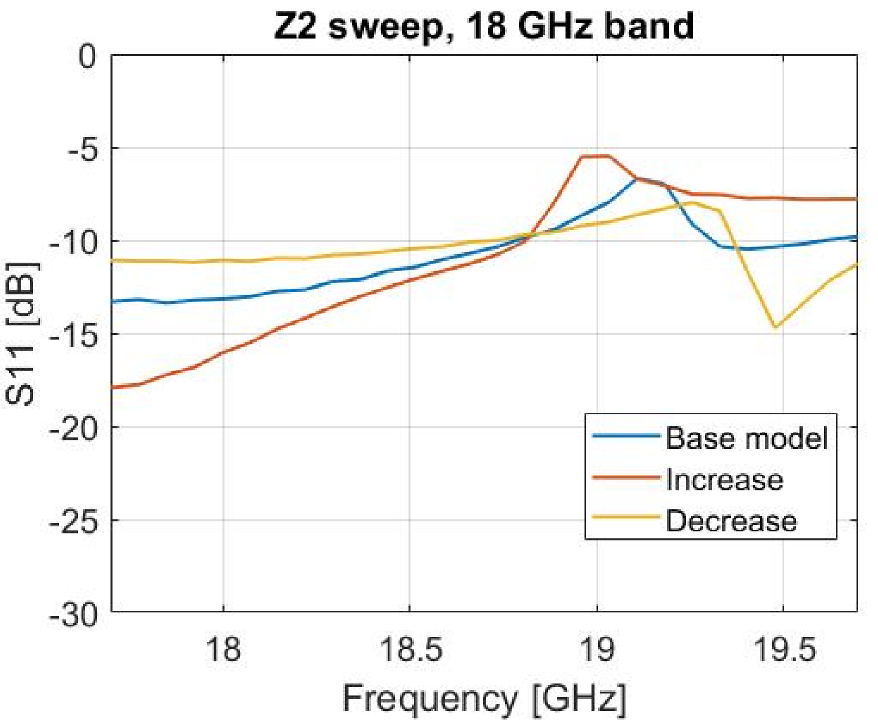

Figure 3.9: Z2 parameter sweep for 18 GHz band.

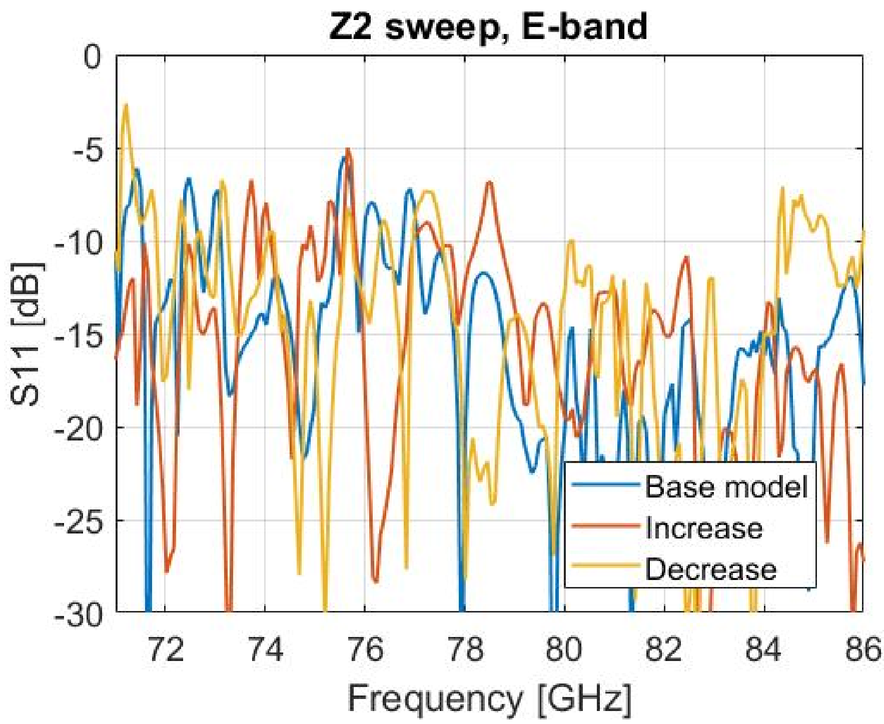

Figure 3.10: Z2 parameter sweep for E-band.

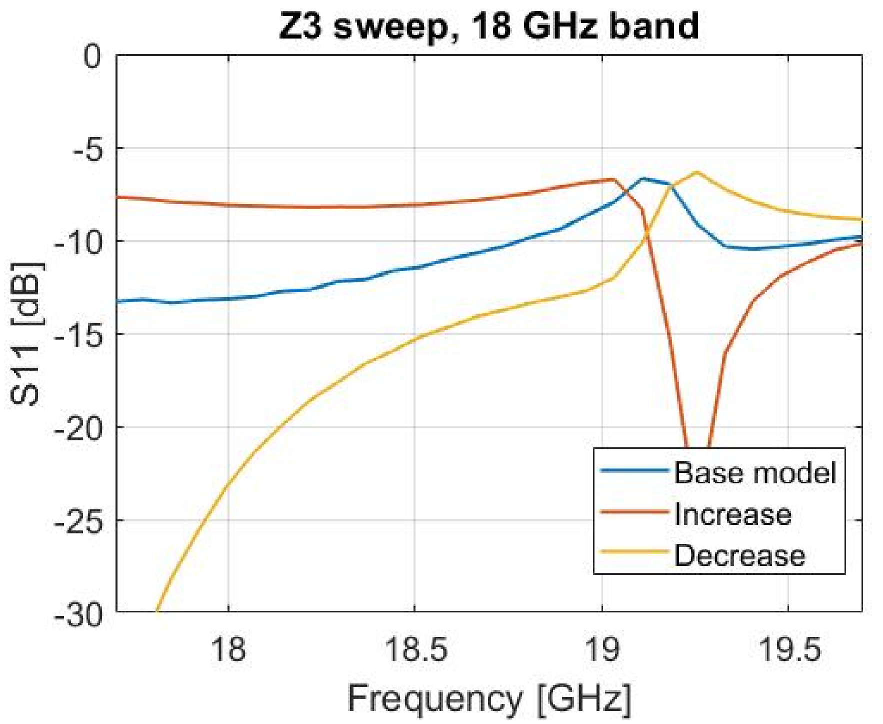

Figure 3.11: Z3 parameter sweep for 18 GHz band.

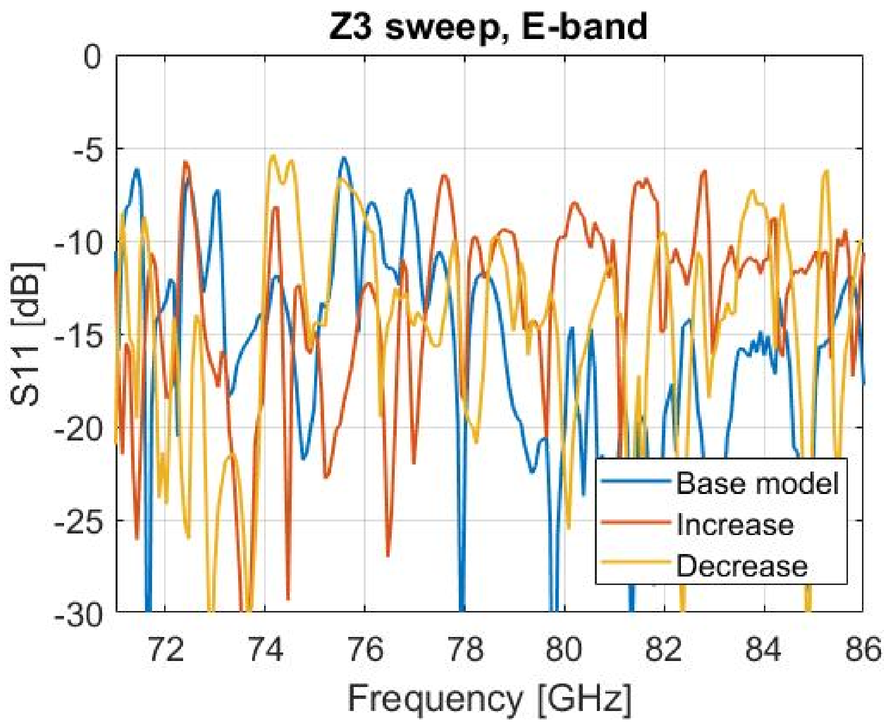

Figure 3.12: Z3 parameter sweep for E-band.

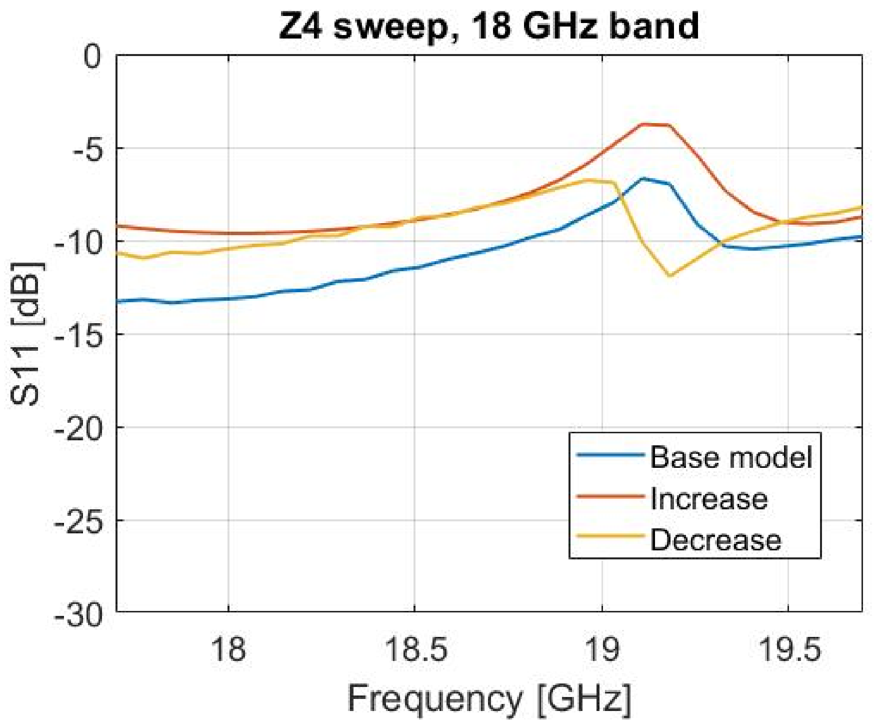

Figure 3.13: Z4 parameter sweep for 18 GHz band.

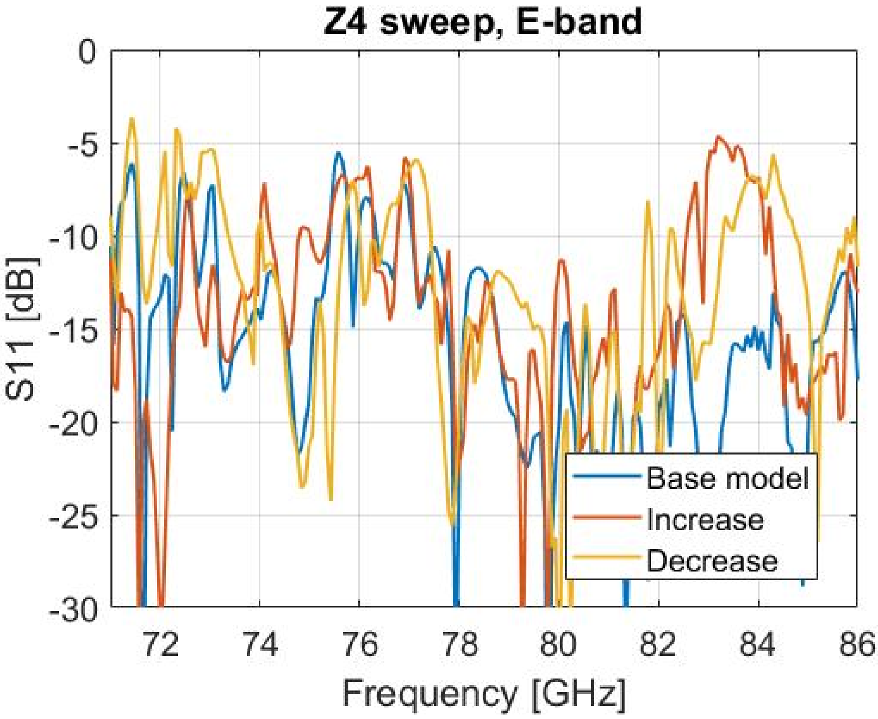

Figure 3.14: Z4 parameter sweep for E-band.

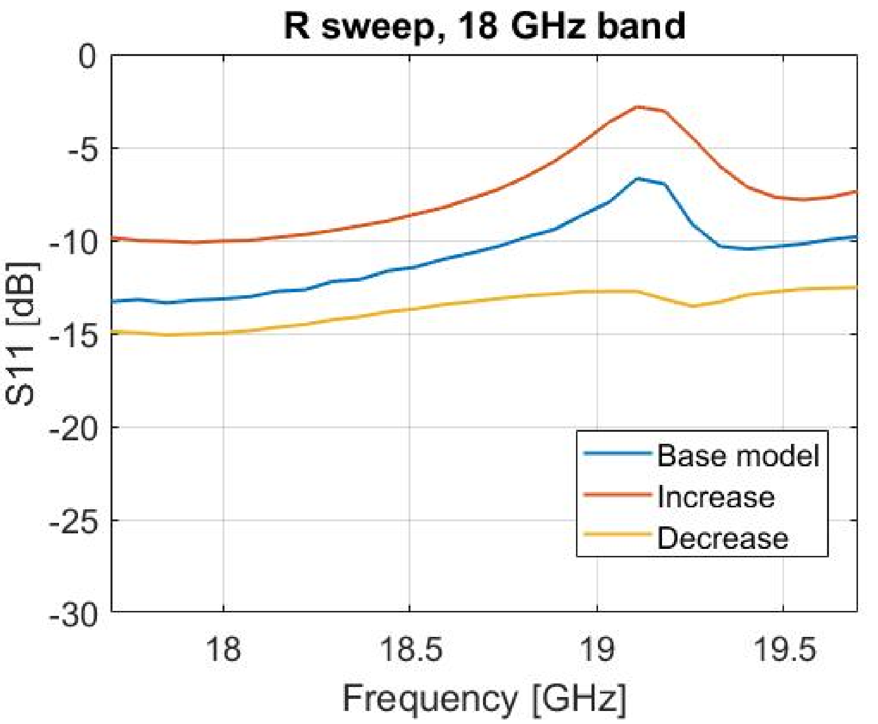

Figure 3.15: R parameter sweep for 18 GHz band.

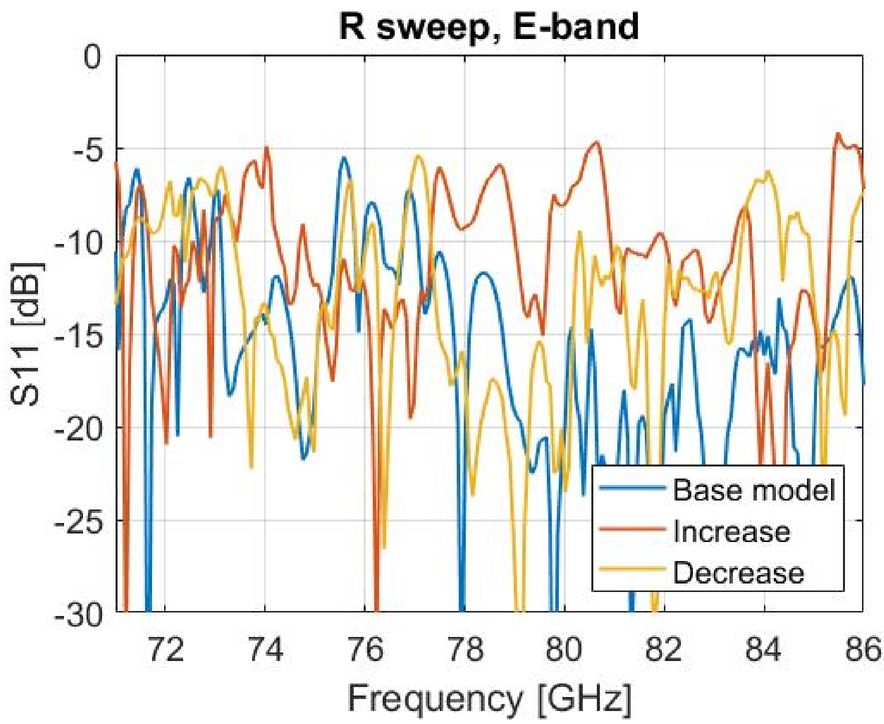

Figure 3.16: R parameter sweep for E-band.

3.2.1.2 Dielectric constant sweep

The results by just changing the dielectric shape was not satisfying. Therefor, a sweep was also done on the dielectric constant to see how it affects the return loss.

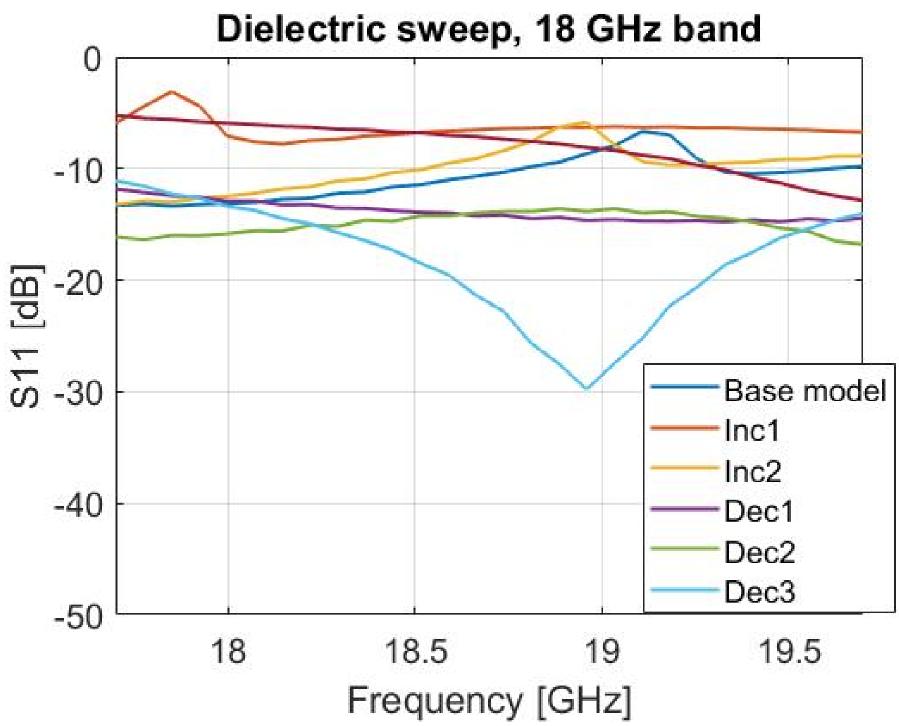

Figure 3.17: Parameter sweep of dielectric constant for 18GHz band.

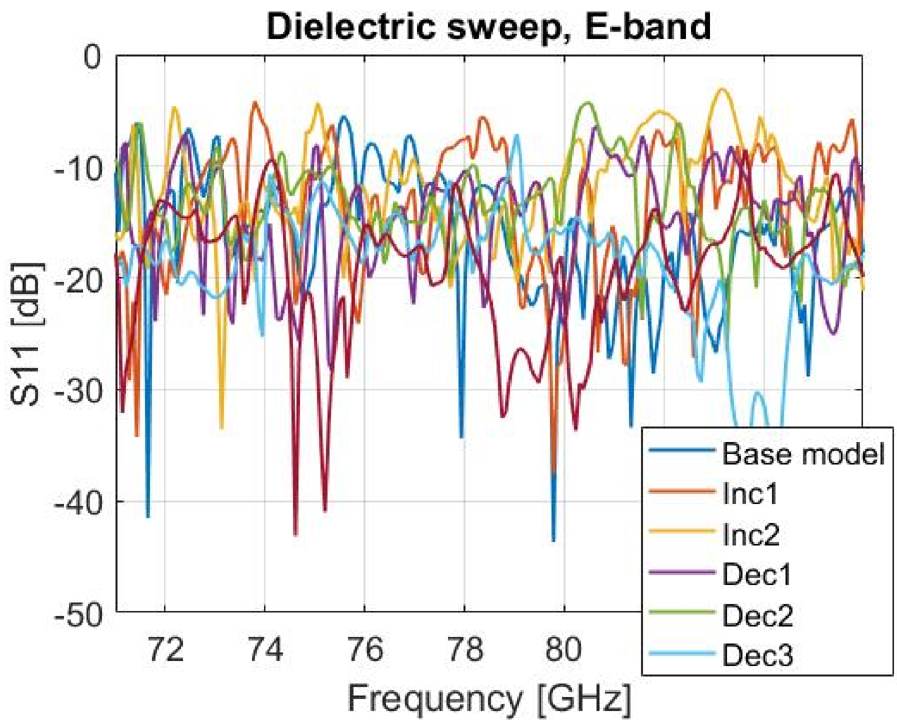

Figure 3.18: Parameter sweep of dielectric constant for E-band.

4

Results

In this chapter, results for the two simulated models will be presented. For each model and frequency; reflection coefficient, radiation pattern, and aperture efficiency will be presented. Model 1, over 18 GHz band and E-band, had a reflection coefficient better than -17 dB and -11 dB respectively. The aperture efficiency was better than 33 % for 18 GHz band and 53 % for E-band. The second model, optimized for 24 GHz and E-band had a reflection coefficient better than -17 dB and -15 dB respectively. The aperture efficiency was better than 53 % for 24 GHz and 44 % for E-band.

4.1 Model 1

The first model is modified and optimized for 18 GHz band and E-band. First the 18 GHz results will be presented, and then the results for E-band. The model is shown in Figure 4.1.

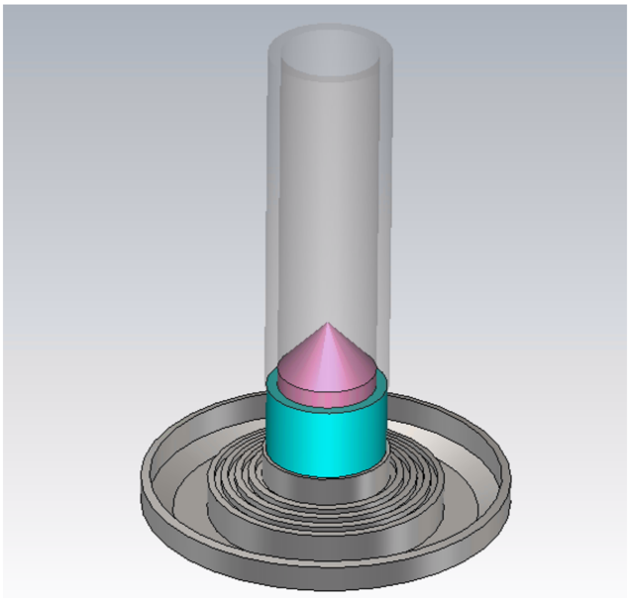

Figure 4.1: Model 1 in CST. The head is divided in two parts, one outer cylinder (blue) with the same material as the original model, and one part inside (pink) the cylinder with a dielectric constant of 1.22

4.1.1 18 GHz band

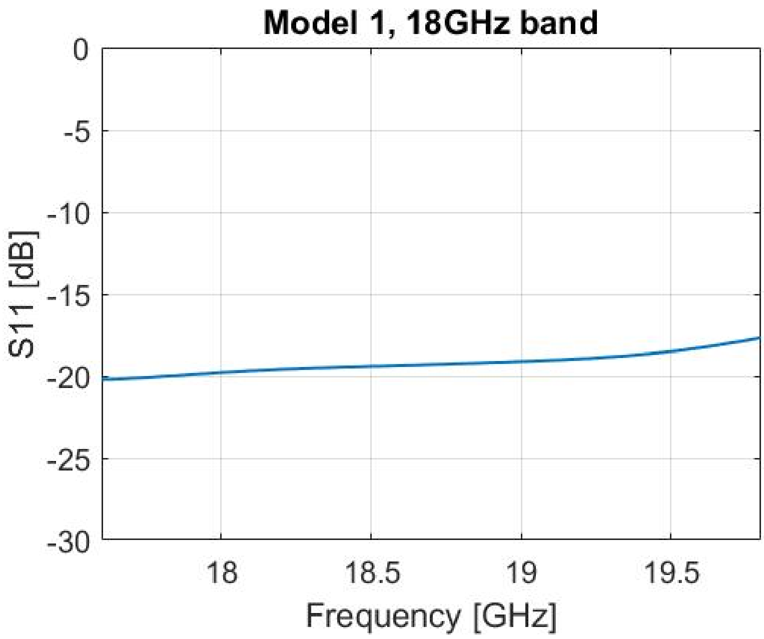

Figure 4.2: Return loss at 18 GHz band.

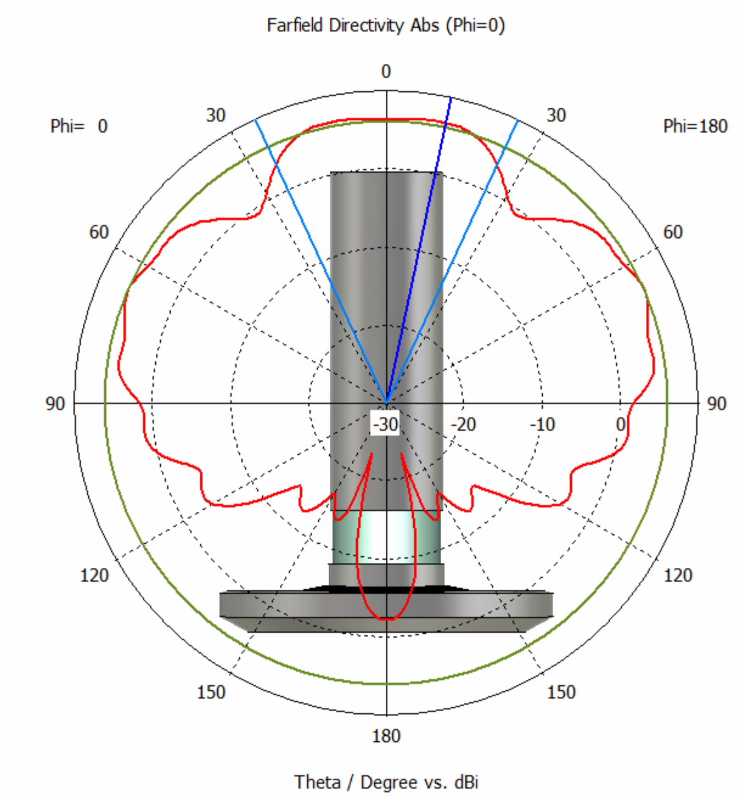

Figure 4.3: E-plane radiation pattern at 18 GHz.

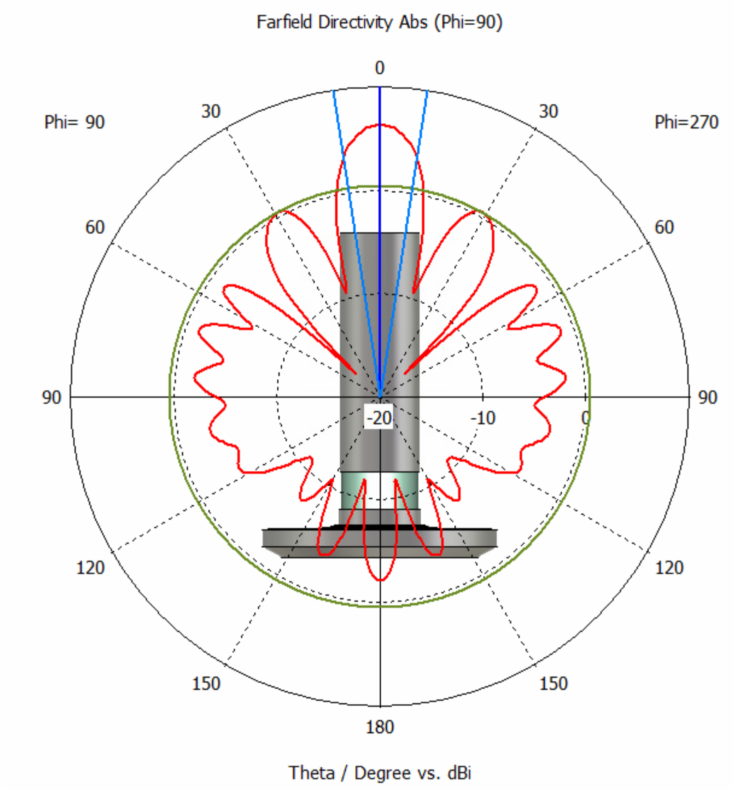

Figure 4.4: H-plane radiation pattern at 18 GHz.

Table 4.1: Efficiencies and total aperture efficiency for model 1 at 18 GHz.

Freq [GHz]	e_{BOR1}	e_{sp}	e_{ill}	e_{pol}	$\boldsymbol{e_{ap}}$
18	99 %	93 %	74 %	48 %	**33%**

4.1.2 E-band

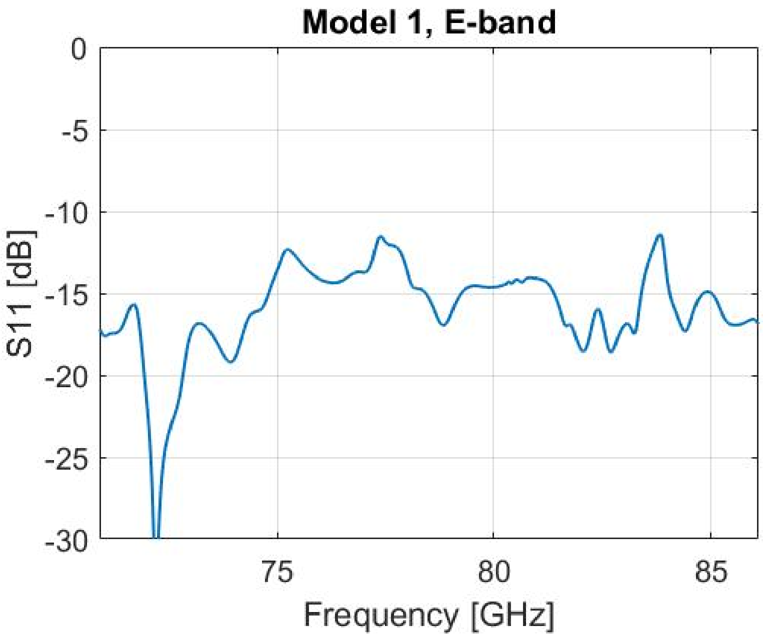

Figure 4.5: Return loss at E-band.

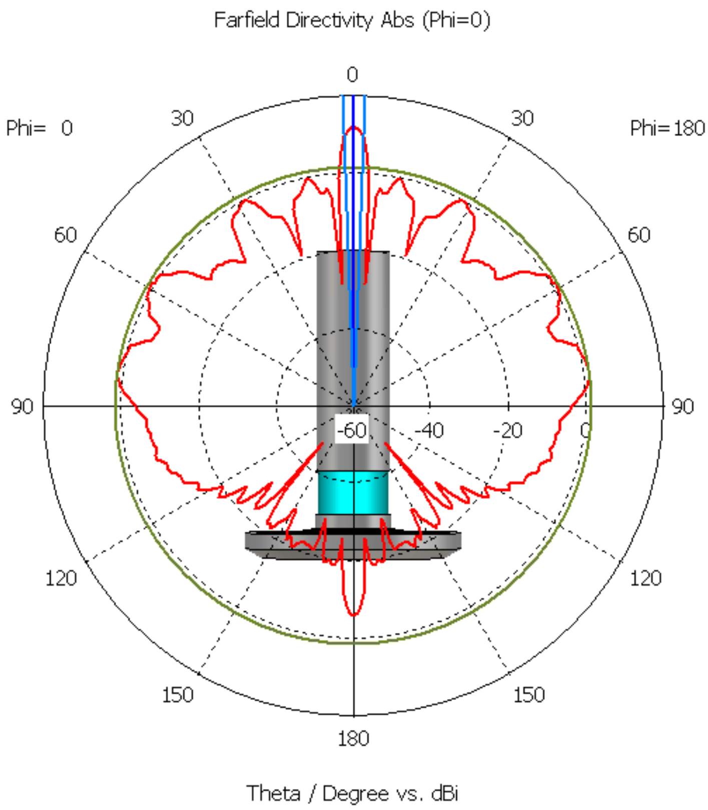

Figure 4.6: E-plane radiation pattern at 71 GHz.

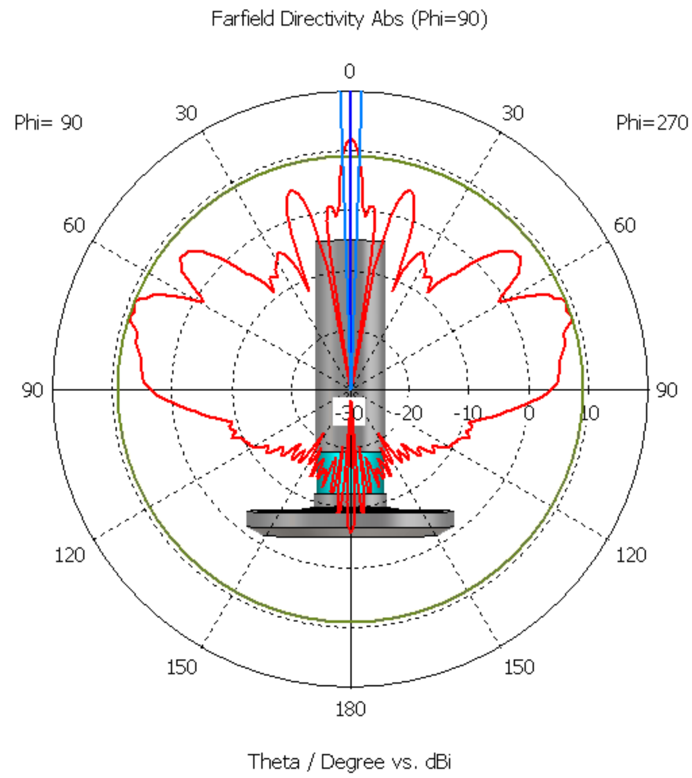

Figure 4.7: H-plane radiation pattern at 71 GHz.

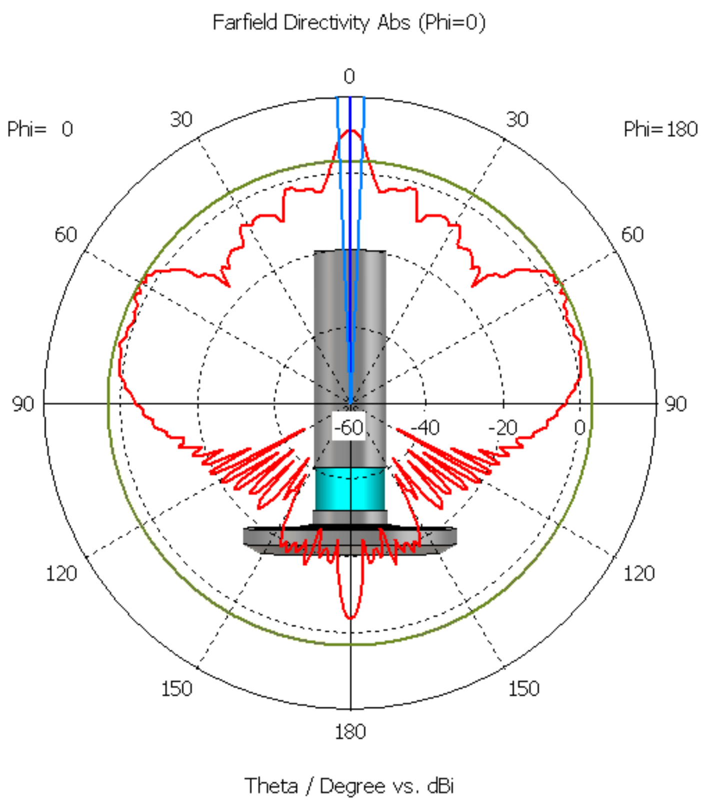

Figure 4.8: E-plane radiation pattern at 81 GHz.

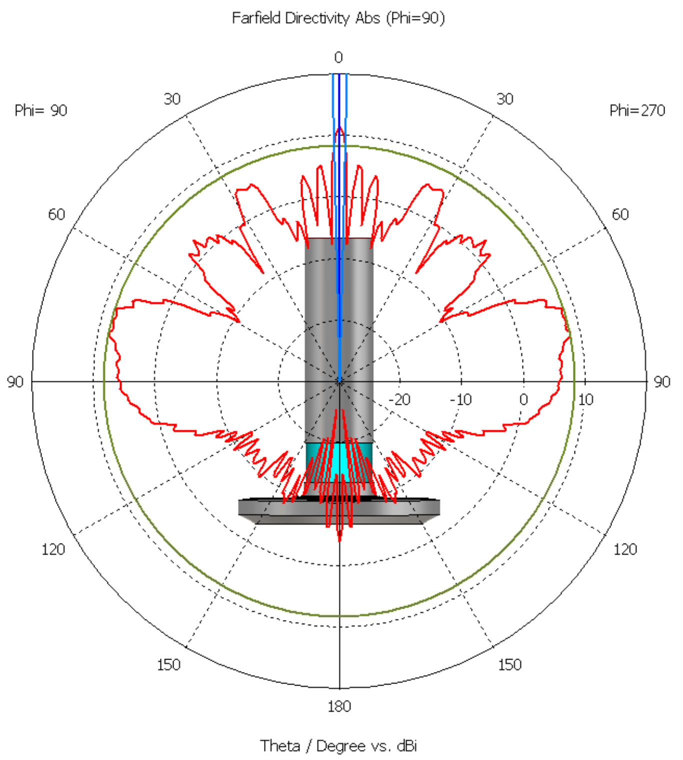

Figure 4.9: H-plane radiation pattern at 81 GHz.

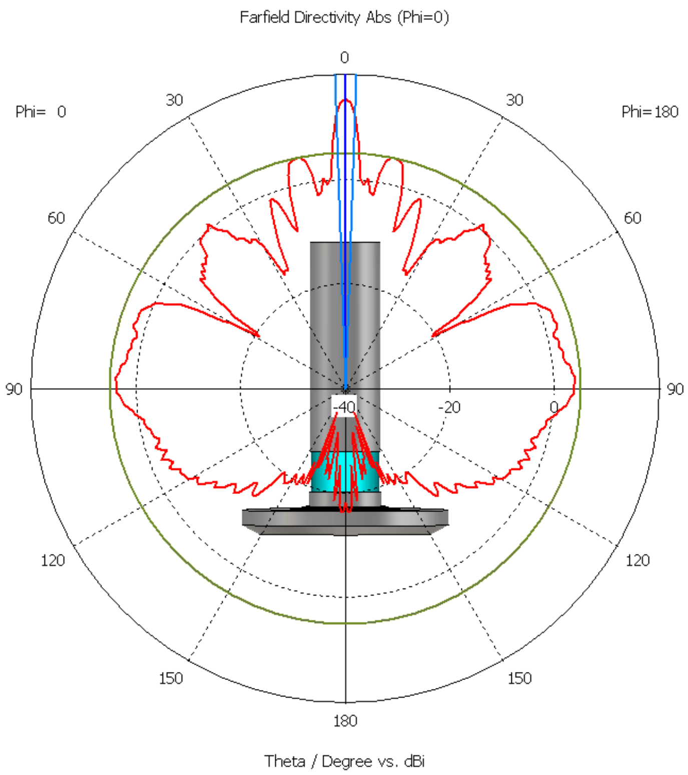

Figure 4.10: E-plane radiation pattern at 86 GHz.

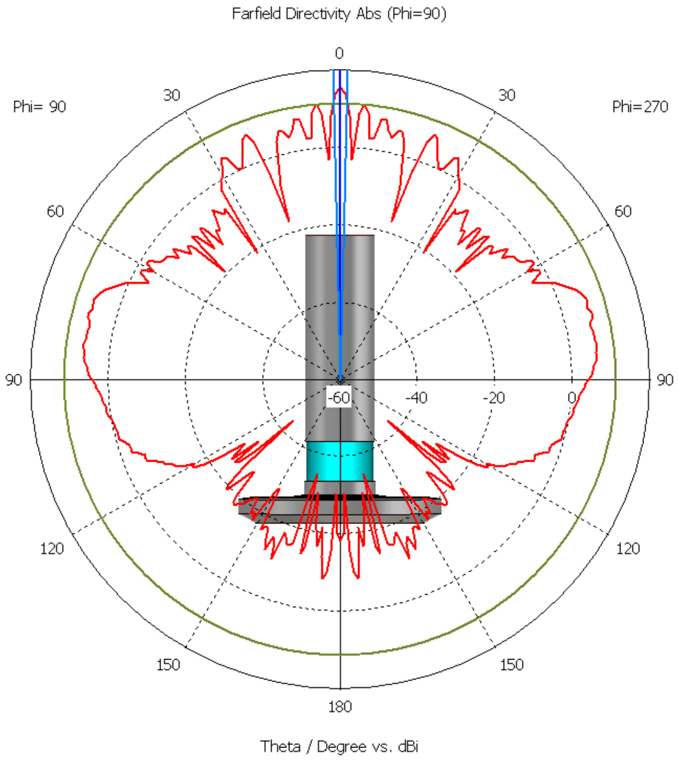

Figure 4.11: H-plane radiation pattern at 86 GHz.

Table 4.2: Efficiencies and total aperture efficiency for model 1 at E-band.

Freq [GHz]	e_{BOR1}	e_{sp}	e_{ill}	e_{pol}	$\boldsymbol{e_{ap}}$
71	95 %	94 %	78 %	88 %	**61%**
81	87 %	95 %	79 %	81 %	**53%**
86	82 %	98 %	74 %	92 %	**55%**

4.2 Model 2

Model 2 is optimized for dual-band with 24 GHz and E-band. First the 24 GHz results will be presented, and then the results for E-band. The model is shown in Figure 4.12. This model differ in two ways compared to model 1. Firstly the head has different dimensions, and secondly the whole head has the same dielectric constant, 1.22. First, the

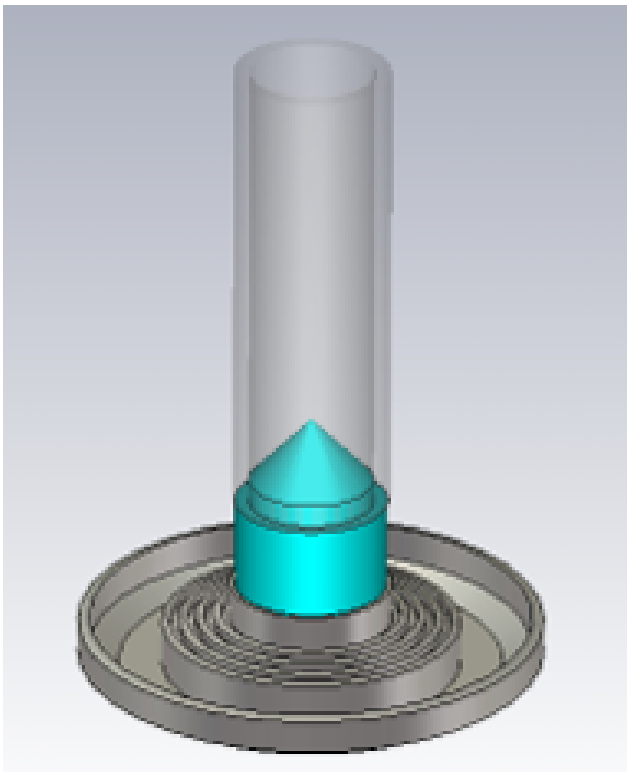

Figure 4.12: Model 2 in CST. The head has a dielectric constant of 1.22.

4.2.1 24 GHz band

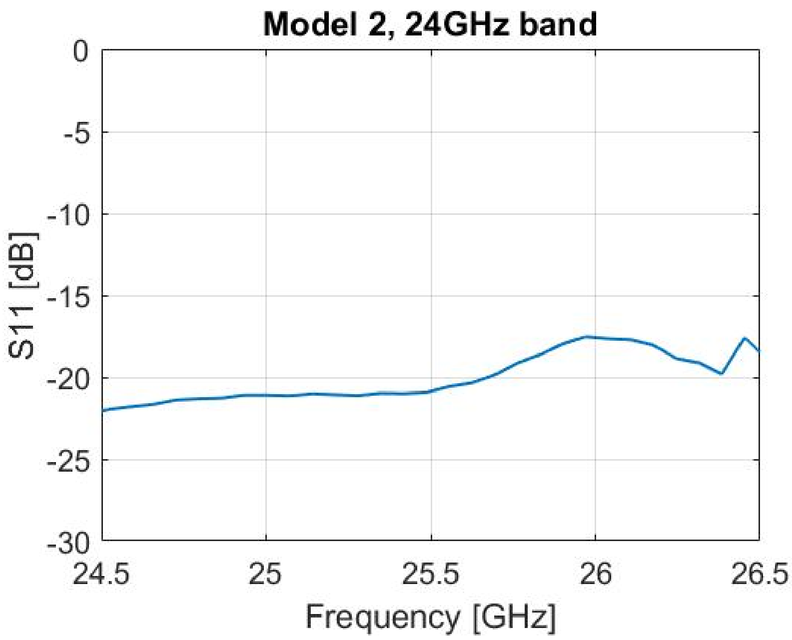

Figure 4.13: Return loss at E-band.

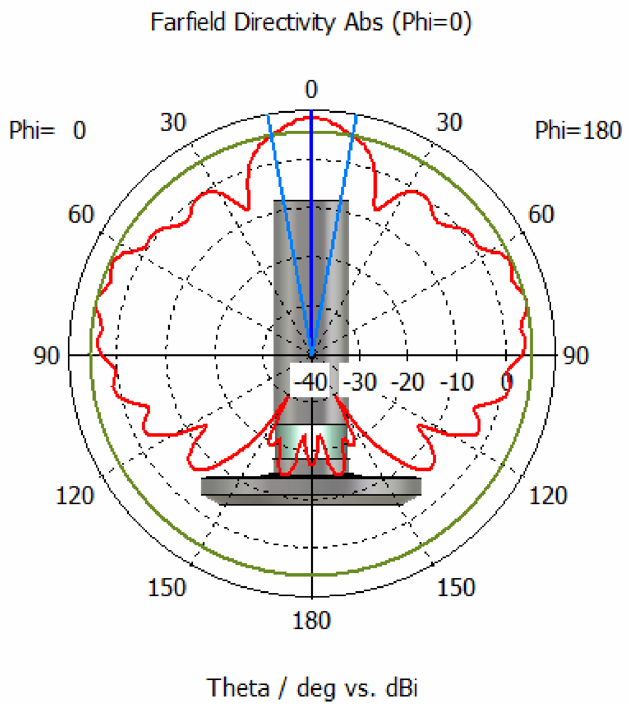

Figure 4.14: E-plane radiation pattern at 24.5 GHz.

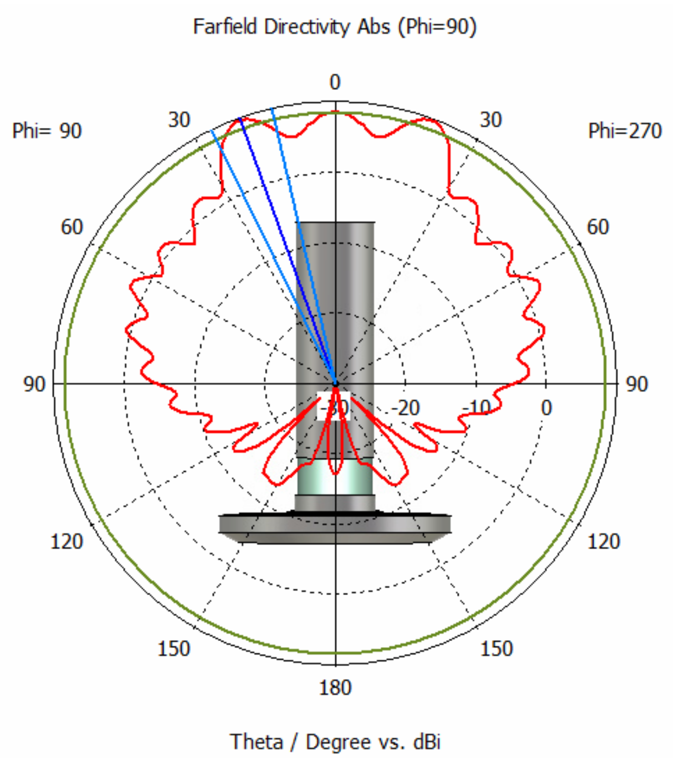

Figure 4.15: H-plane radiation pattern at 24.5 GHz.

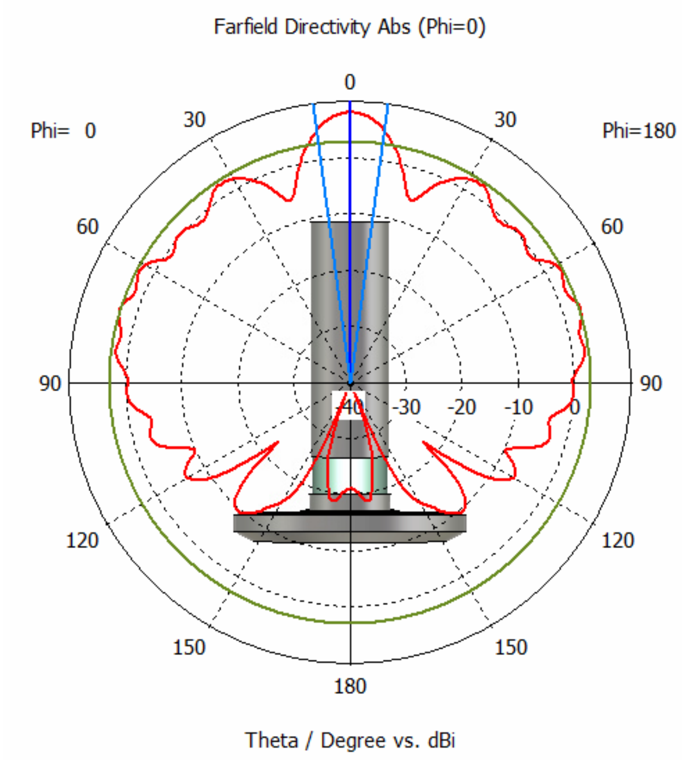

Figure 4.16: E-plane radiation pattern at 26.5 GHz.

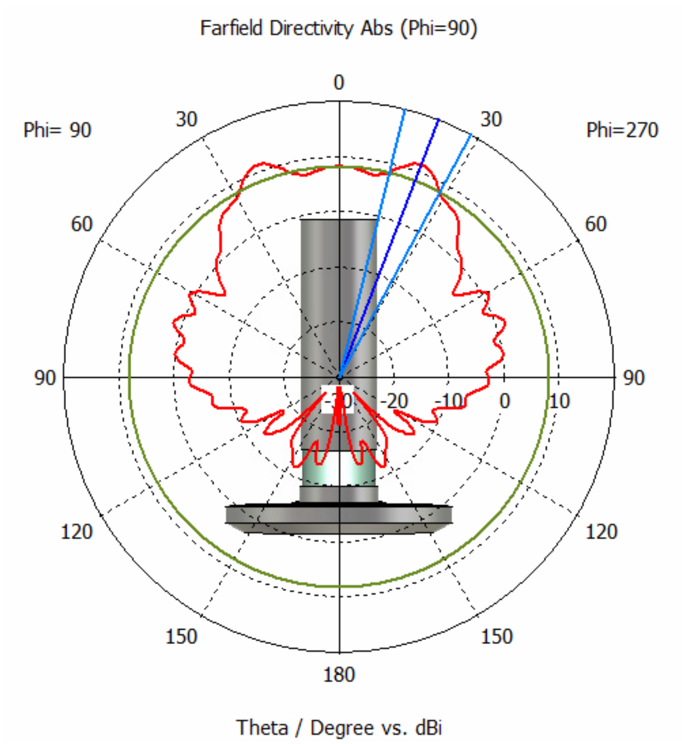

Figure 4.17: H-plane radiation pattern at 26.5 GHz.

Table 4.3: Efficiencies and total aperture efficiency for model 2 at 24 GHz band.

Freq [GHz]	e_{BOR1}	e_{sp}	e_{ill}	e_{pol}	$\boldsymbol{e_{ap}}$
24.5	99 %	97 %	76 %	76 %	**56%**
26.5	99 %	98 %	65 %	83 %	**53%**

4.2.2 E-band

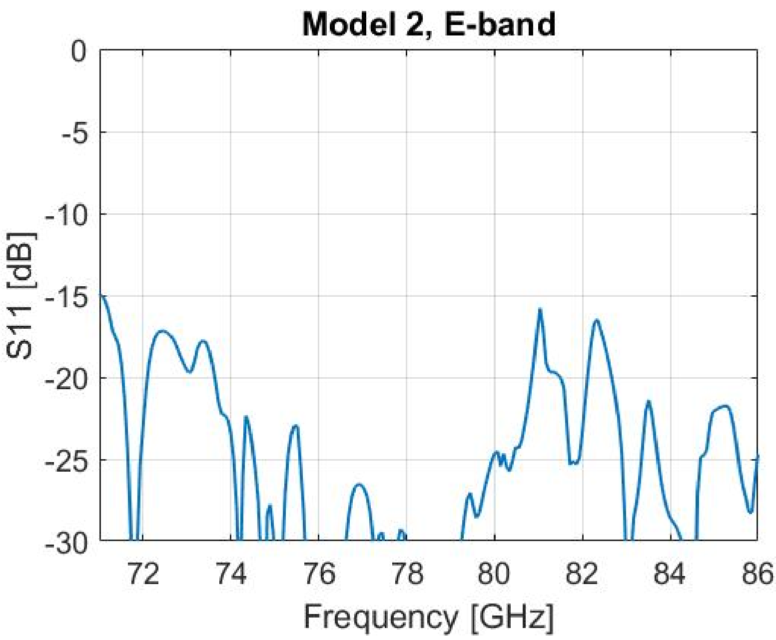

Figure 4.18: Return loss at E-band.

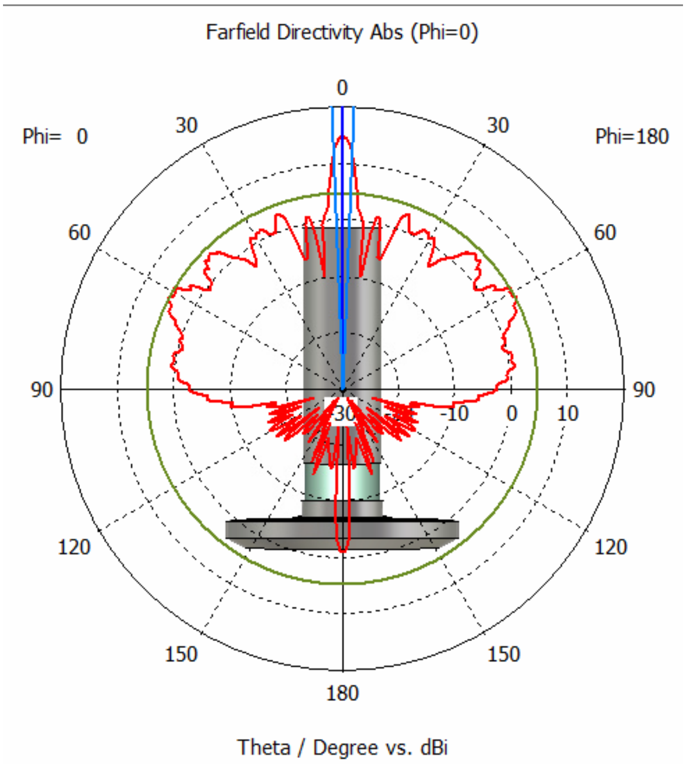

Figure 4.19: E-plane radiation pattern at 71 GHz.

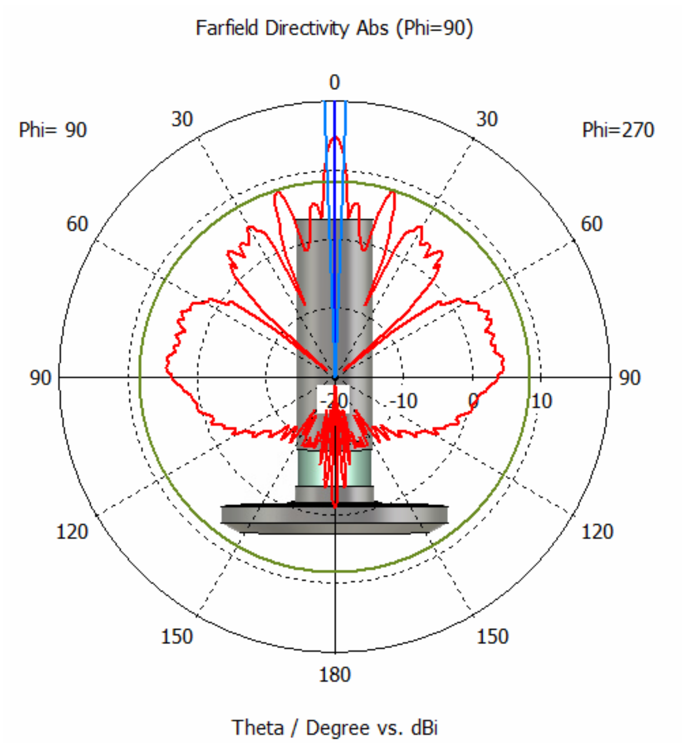

Figure 4.20: H-plane radiation pattern at 71 GHz.

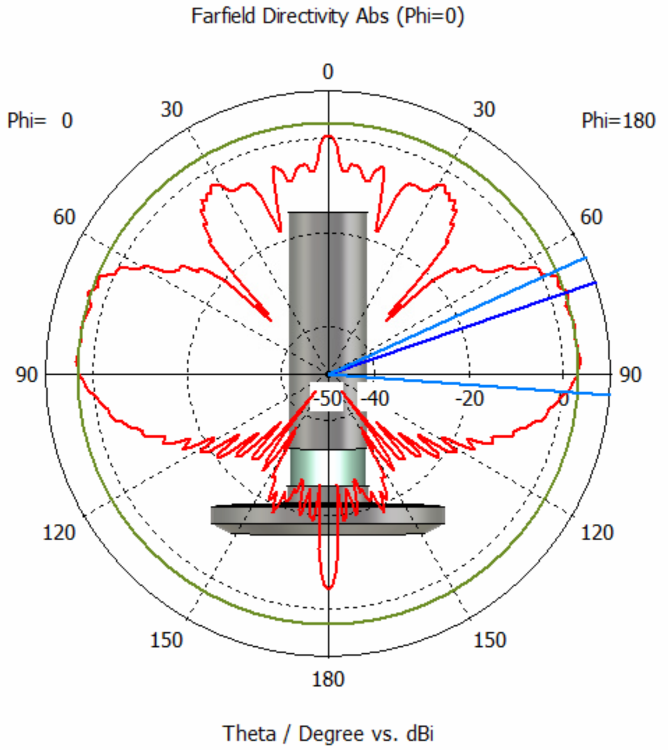

Figure 4.21: E-plane radiation pattern at 81 GHz.

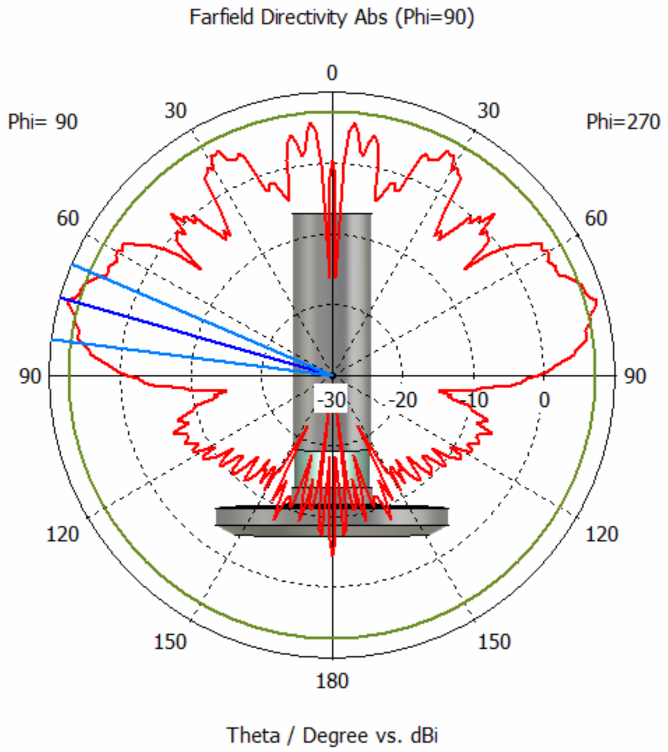

Figure 4.22: H-plane radiation pattern at 81 GHz.

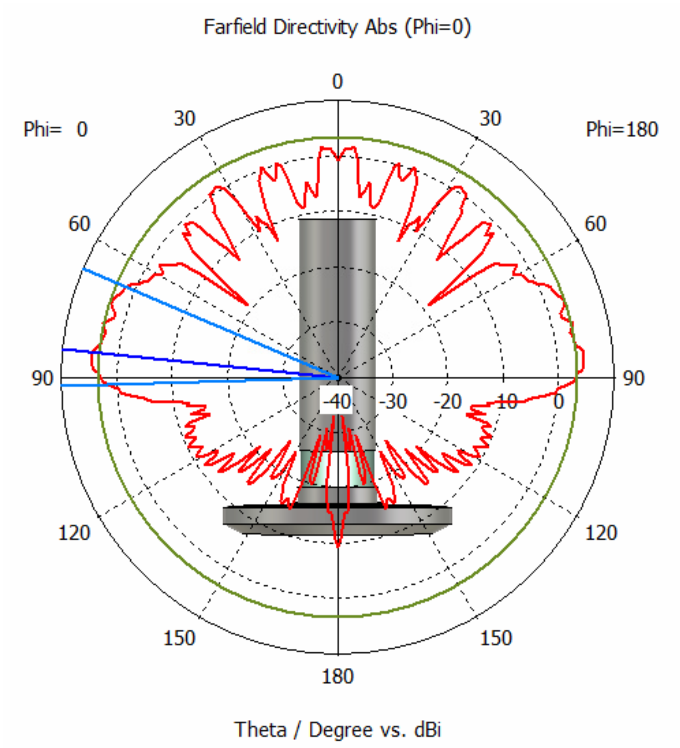

Figure 4.23: E-plane radiation pattern at 86 GHz.

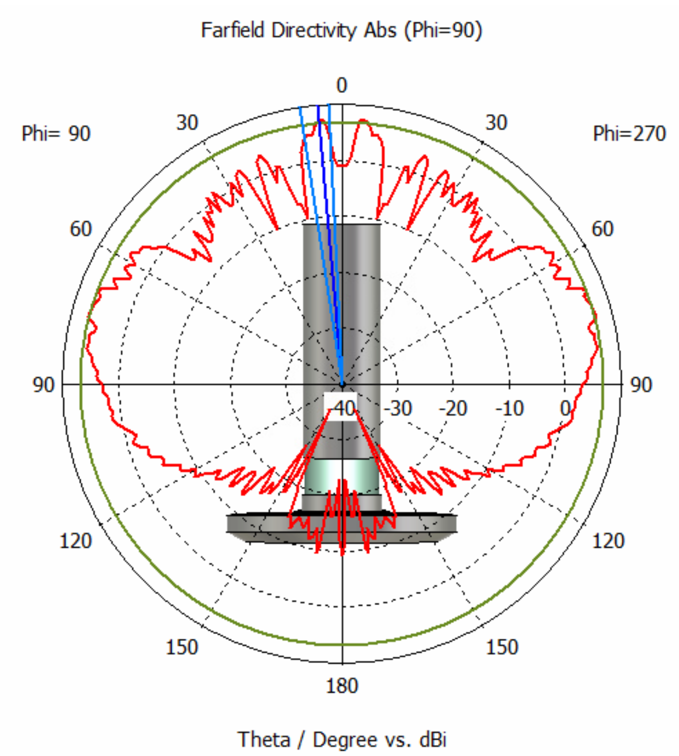

Figure 4.24: H-plane radiation pattern at 86 GHz.

Table 4.4: Efficiencies and total aperture efficiency for model 2 at E-band.

Freq [GHz]	e_{BOR1}	e_{sp}	e_{ill}	e_{pol}	$\boldsymbol{e_{ap}}$
71	95 %	95 %	73 %	68 %	**45%**
81	87 %	98 %	62 %	84 %	**44%**
86	80 %	97 %	72 %	88 %	**49%**

5

Discussion and conclusion

5.1 Modeling process

The strategy of sweeping parameters was a good start to get a feeling for how changes of the dielectric head structure affects the return loss. However, a distinct tendency could not always be found. To get a deeper understanding, the field changes could have been studied.

5.2 Results

None of the models in this project fulfills the requirements that was stated in the beginning of the work. The bad polarization efficiency for 18 GHz band of model 1 was introduced when the separation of the dielectric head was done, which intuitively is a bit surprising. This trouble could have been further investigated. Regarding model 2, it has promising simulation results. The challenge here is to find a way to manufacture the dielectric head with a dielectric constant of 1.22. This could be done by using a material with higher dielectric constant, but mixed with air. Either by drilling holes in the structure, or using other shapes like a cross-structure.

5.3 Further work

Manufacturing was outside the scope of this project. However, it would have been good to verify the results, especially on Model 2. With this comes the challenge with realizing a material with the dielectric constant 1.22. Another thing to look further into is why the polarization is bad for 18 GHz band of model 1. A deeper study on how the parameter changes effects the fields would also be something to look at in the future.

5.4 Conclusion

In conclusion, this thesis has showed that it is theoretically possible to model a dual band hat feed with promising performance. However, the models presented here are hard to realize.

Bibliography

[1] D. K. Cheng, *Field and wave electromagnetics: New International Edition*, 2nd ed. Harlow: Pearson, 2014, ISBN: 9781292026565.

[2] D. Pozar, *Microwave engineering*, 4th ed. Hoboken, NJ: Wiley, 2012, pp. 6–44, 95–161, ISBN: 9780470631553.

[3] P.-S. Kildal, “The hat feed: A dual-mode rear-radiating waveguide antenna having low cross polarization”, *IEEE Transactions on Antennas and Propagation*, vol. 35, no. 9, pp. 1010–1016, 1987.

[4] M. R. Arild Moldsvor and P.-S. Kildal, “An efficient rectangular hat feed for linear polarization and low sidelobes”, IEEE Antennas.

[5] O. J. Hansen A. Kishk P.S.Kildal, “High performance reflector hat antenna with very low sidelobes for radio-link applications”, pp. 893–896, Jun. 1995.

[6] P. K. J. Yang, “Fdtd design of a chinese hat feed for shallow mm-wave reflector antennas”, pp. 2046–2049, Jun. 1998.

[7] M. Yousefnia, A. Pirhadi, M. Hakkak, “Analysis and design of parabolic hat feed antenna,“ Proc. 2005 Int. Symp., 3–8 July 2005, vol. 3A, pp. 650–653.

[8] M. Denstedt, T. Ostling, J. Yang,P.-S. Kildal, “Tripling bandwidth of hat feed by genetic algorithm optimization,“ IEEE AP-S 2007 Symp., Hawai, 10–15 June 2007.

[9] Wei Wei, Jian Yang, Tomas Östling and Thomas Schafer, “A new hat feed for reflector antennas realized without dielectrics for reducing manufacturing cost and improving reflection coefficient”, IET Microwaves Antennas Propagat, vol. 5, no. 7, pp. 837-843, July, 2011.

[10] J. Yang, P.-S. Kildal, ”Gaussian vertex plate improves return loss and far-out sidelobes in prime-focus reflector antennas,” Microw. Opt. Tech. Lett, 1999, 21, (2), pp. 125–129.

[11] Erik G. Geterud, Jian Yang, Tomas Ostling, and Pontus Bergmark, “Design and optimization of a compact wideband hat-fed reflector antenna for satellite communications”, IEEE Trans. Antenna Propagat., vol. 61, no. 1, pp. 125–133, 2013.

[12] P.S. Kildal, A. Haddadi and Jian Yang, “Numerical Validation of Arecibo-Based Analytical Hat Antenna Theory Using Canonical PEC/PMC Strip Grids”, 2016 IEEE international Symp. on Antennas Propag (APS), Puerto Rico, June 2016.

[13] E. Geterud, J. Yang and T. Ostlingy, “Radome Design for Hat-Fed Reflector Antenna”, 6th Eur. Conf. on Antennas Propagat. (EuCAP2012), Prague, 26-30 March 2012.

[14] J. Yang, W. Wei, T. Ostlingy, T. Schafer, “A new metal-rod-supported hat antenna for potentially combining with the Eleven antenna as a dual-band feed for reflectors”, In 5th Eur. Conf. on Antennas Propagat. (EuCAP2011), Rome, Italy, 11 - 15 April 2011.

[15] J. Yang and P.-S. Kildal, “Calculation of ring-shaped phase centers of feeds for ring-focus paraboloids”, *IEEE Transactions on Antennas and Propagation*, vol. 48, no. 4, pp. 524–528, 2000.

[16] T. O. Erik Geterud Jian Yang, “Radome design for hat-fed reflector antenna”,

[17] P.-S. Kildal and Z. Sipus, “Classification of rotationally symmetric antennas as types and ,” IEEE Antennas Propag. Mag., vol. 37, no. 6, Dec. 1995.

[18] P.-S. Kildal, J. Yang and M. Ivashina, “New BOR1 and decoupling efficiencies for characterizing ultra-wideband reflectors and feeds for future radio telescopes“, In 5th Eur. Conf. on Antennas Propagat. (EuCAP2011), Rome, Italy, 11 - 15 April 2011.

[19] J. Yang, S. Pivnenkoy and P.-Simon Kildal, “Comparison of two decade-bandwidth feeds for reflector antennas: the Eleven antenna and quadridge horn“, In 4th Eur. Conf. on Antennas Propagat. (EuCAP2010), Barcelona, Spain, 12 - 16 April 2010.

[20] P.-S. Kildal, “Factorization of the feed efficiency of paraboloids and cassegrain antennas”, *IEEE transactions on antennas and propagation*, vol. 33, no. 8, pp. 903–908, 1985.

[21] D. M. Sullivan, *Electromagnetic Simulation Using the FDTD Method, 2nd Edition.* Harlow: John Wiley Sons, 2013.

[22] Z. Chen, J. Yiang and P.-S. Kildal, “Design of sector antenna with wideband 2d hat-fed reflector for wireless communications”, in 2015 International Symposium on Antennas and Propagation, 9-12 November 2015, Hobart, Tasmania, Australia.